# Accurate crystal structures of $C_{12}H_9CN$, $C_{12}H_8(CN)_2$, and $C_{16}H_{11}CN$ valence isomers using non-spherical atomic scattering factors

Nathan D. D. Hill,[1,2] Elaura Lilienthal,[1,2] Christopher O. Bender[1] and René T. Boeré*[1,2]

[1] Department of Chemistry and Biochemistry, University of Lethbridge, 4401 University Dr. W, Lethbridge, AB, Canada T1K 3M4

[2] The Canadian Centre for Research in Advanced Fluorine Technologies (C-CRAFT), University of Lethbridge, 4401 University Dr. W, Lethbridge, AB, Canada T1K 3M4

Corresponding author: Prof. René T. Boeré (email: boere@uleth.ca)

Journal: Journal of Organic Chemistry

Manuscript ID: Accepted Manuscript jo-2022-017068

**Abstract**

Fourteen crystal structures, mostly from good quality datasets but including some marginal and twinned exemplars, from a series of novel polycyclic benzo- and naphtho-fused organic nitriles are presented and accurately described, including some related structures of a bromo-substituted and partially hydrogenated analogs. These structures represent a considerable increase in the number of published structures within their archetypes. This work highlights the significant advancement in structural refinement software proffered by NoSpherA2, which enables Hirshfeld Atom Refinement (HAR) of the structures within Olex2 v1.5. This results in determination of C-H bond lengths with accuracy near to neutron diffraction values at far lower experimental cost, and an average improvement in C-C bond precision of 42% compared to Independent Atom Model refinements. H-atoms (apart from disordered components) refined well with anisotropic displacement parameters. Non-classical H-bonding (C–H···N≡C) in this series is analyzed, and dipolar nitrile-nitrile interactions (C≡N···C≡N) in three major motifs described by Wood et al. (Acta. Cryst. B, 2008, 64, 393-396) are found in 9 out of 13 nitrile-containing compounds of this series, a much higher proportion than the global average of 21% of nitrile-containing compounds. The HAR/NoSpherA2 approach shows increasing benefits with better data quality without apparent discontinuities.

## INTRODUCTION

There is continuing strong interest in the preparation and applications of benzobarrelenes (1,4-dihydro-1,4-ethenonaphthalenes, **I** in Chart 1),[1-6] which are derivatives of the parent barrelene (*bicyclo*[2,2,2]-2,5,7-octatriene) first reported by Zimmerman in 1960.[7] Benzobarrelenes are particularly suited as chelating bis-$\eta^2$-ethene ligands for low-valent transition metals, such that more than 70% of the 117 reported crystal structures in the Cambridge Structure Database (CSD, version 2021.2)[8] are of such complexes. Schlesinger et al. devised synthetic strategies for an impressive range of partially halogenated benzobarrelene derivatives which can then be further functionalized.[3] Rhodium complexes of such benzobarrelenes are highly efficient catalysts for 1,4-addition of phenylboronic acid to 2-cyclohexen-1-one. Marder et al. have developed a hexadehydro-Diels-Alder (HDDA) reaction in which substituted benzobarrelenes and barrelene-like compounds with extended ring systems can be synthesized from a benzyne-trapping reaction with an aromatic reagent (benzene, toluene, anthracene).[1] Fluorinated benzobarrelenes have also recently been reported.[2] In all, about 20 structures of type **I** (Chart 1) have been reported, excluding metal coordination complexes and those embedded into additional rings. We have provided one of these entries in a previous report on a fully saturated tetrabromobenzobarrelene and 2,3-dibromo-1,4-ethenonaphthalene which is derived from the former by double dehydrobromination.[9]

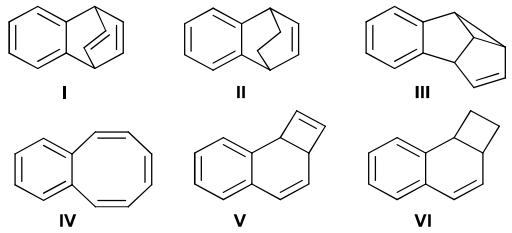


**Chart 1**

Selective saturation of the alkene 'staves' of benzobarrelenes is possible.[10] Dihydrobenzobarrelenes (1,4-dihydro-1,4-ethanonaphthalenes, **II** in Chart 1) are of interest as spacers between antipodal redox sites[11] or as a vector to benzannulation via the Alder-Rickert reaction involving thermolytic removal of the saturated stave of the barrelene.[12-14] About 20 crystal structures of type **II**, excluding metal coordination complexes and embedded rings, are reported in the CSD. However, all but four of these are affected by positional disorders between the 'saturated' and 'unsaturated' barrelene staves, frustrating explorations of a structure correlation principle for the Alder-Rickert reaction.[6] Additional ordered crystal structures of type **II** are therefore highly desirable.

Benzosemibullvalenes (2*a*,2*b*,6*b*,6*c*-tetrahydro-1,2*b*,3,6-tetramethylbenzo(*a*)cyclopropa(*c,d*)pentalenes, **III** in Chart 1), are benzofused derivatives of tricyclo[3.3.0.$0^{2,8}$]octa-3,6-dienes. They represent a polycyclic system with dramatic ring strain that has attracted modern structural research interest and are most often the product of the photolytic rearrangement of benzobarrelenes.[15-19] Sajimon et al. demonstrated that there is a degree of regioselective control in this rearrangement based on the steric bulk of substituents on the benzobarrelene.[20] There have also been successful attempts to synthesize benzosemibullvalenes by conventional means, by either dehydrobromination[21] or by thermolytic isomerization of perphenylbutenyne which proceeds through formation of an intermediate carbene compound via a reverse Skattebøl rearrangement.[22] Despite the intrinsic interest in such strained structures, fewer than

ten exemplars of type **III**, excluding metal complexes and embedded rings, could be retrieved from the CSD.

Cyclooctatetraenes (COTs) are anti-aromatic [8]-annulenes with a distinctly non-planar geometry which see a great deal of use in coordination chemistry as sterically demanding ligands.[23-24] There has been strong directed research in recent years towards geometric modifications of polycyclic arenes to modulate electronic and optical properties that arise from three-dimensional nanocarbon structures.[25-31] COTs are an essential component to introducing stable and rational curvature into polycyclic sheets due to their tub-shaped geometry, and to this end there has been significant inquiry as to how to incorporate COTs into these systems. In pursuit of this goal, Bello-Garcia et al. have contributed a large number of easily accessible functionalized benzocyclooctatetraenes, BCOTs (benzo[8]annulenes, **IV** in Chart 1), via Ru-catalyzed [2+2+2] cycloaddition of arylenynes to dihydrobiphenylenes followed by a straightforward ring opening reaction.[32] Even with this significant contribution, structures of simple BCOTs remain rare, with only 11 structures currently reported in the CSD.

Although there has been an overall decline in the prevalence of photochemistry since the 1990s, there has been continued interest in the production of highly strained polycyclic systems which have well-established photosynthetic methods but are difficult to access through conventional chemical means. 2*a*,8*b*-dihydrocyclobuta[*a*]naphthalenes, DCBNs, (**V** in Chart 1), are benzannulated derivatives of bicyclo[4.2.0]octa-2,4,7-triene and belong to this category. Much of the recent research in this area is directed towards DCBN systems containing embedded rings,[33-39] but for accuracy the geometry comparisons in this work will focus on just three DCBN crystal structures without embedded rings deposited in the CSD to date.

Partly saturated derivatives of **V** are the 1,2,2*a*,8*b*-tetrahydrocyclobuta[*a*]naphthalenes, TCBNs, (**VI** in Chart 1), benzannulated derivatives of bicyclo[4.2.0]octa-2,4-dienes. These have been explored in recent literature by several groups investigating the fundamental reactivity and modification of synthetic stereo- and regioselectivity of the archetypical photoreaction of naphthalenes with substituted alkenes to form TCBNs.[40-45] There are 12 TCBN crystal structures without embedded rings deposited in the CSD to date.

One of us produced a rich set of related compounds from a lengthy research programme in mechanistic photochemistry, composed of unusual valence isomers that are the products of excited-state reactions.[10, 46-50] A treasure trove of crystals are now available, mostly of suitable quality for single crystal X-ray diffraction, and their crystal and molecular structures are reported herein. In all, 14 structures of types **I** – **VI** (Chart 1) are reported (including two naphtho-fused analogs), mostly mono- or dinitriles, and of which only one of type **VI** was previously reported but with a different space group and no record of fractional atom coordinates.[51] These structures significantly expand the number of accurately characterized 3D geometries for such hydrocarbon cage compounds, for example in the case of **III**, our work constitutes a 30% increase in reported SC-XRD geometries, and for **V** an increase of 67%.

Several important publications, and methodologies, have appeared over the past decade, which reported the ability to refine H-atom positions accurately, and anisotropic displacements, even with 'standard' resolution SC-XRD data [$\sin(\theta)/\lambda \approx 0.6$ Å$^{-1}$] by using the so-called Hirshfeld atom refinement (HAR) approach.[52-54] However, the uptake by chemical crystallographers, as judged from the citation literature, has been modest. Recently, a user-friendly integration of several very efficient modern density functional theory (DFT) computation packages with the olex2.refine engine[55] was implemented in the program NoSpherA2,[56] which is bundled with recent new releases of the popular refinement package Olex2. This

program uses custom atomic scattering factors that are fully polarized to the actual atom positions in the crystal lattice, which permits accurate placement of hydrogen atoms with a precision that approaches that of neutron diffraction, the acknowledged 'gold standard' for light atom structures.[57] Our group has previous experience in the application of the HAR/NoSpherA2 method in the context of organophosphines[58] and copper(II) sulfates.[59] The impetus for adopting these HAR approaches is that standard resolution data from home labs equipped with area detectors often contain more information than the standard independent atom model (IAM) can exploit. This approach to small-molecule crystallography in no way displaces high-accuracy crystallography using multipole refinements and other cutting-edge quantum crystallography developments,[60-61] nor does it compete with the recent development of spallation neutron sources, which have made single-crystal neutron diffraction more feasible than ever.[62] However, with more than 60 000 new structures added to the CSD and more than 4 000 to the Inorganic Crystal Structure Database each year, the vast majority obtained from home-lab X-ray diffraction experiments, the prospect of improving the accuracy of the majority of structure models is highly attractive.[56]

The promise of routinely refining H-atom parameters is especially welcome with the increased recognition of the importance of London dispersion interactions (the attractive component of the van der Waals potential) on many aspects of chemical interaction and structure. These are overwhelmingly hydrocarbon interactions, ranging from small molecules,[58, 63-68] crystal structure directors,[69] chemical reaction mechanisms,[70] and biological macromolecular interaction mechanisms.[71] A dispersion energy donor scale has recently been proposed.[72] There is now even direct evidence for CH···HC 'bonding' with the shortest approach of 1.566(5) Å in crystals of tri(3,5-*tert*butylphenyl)methane at 20 K.[73]

The ongoing interest in weak intermolecular interactions in the ever-growing field of 'crystal engineering' will also benefit from accurate treatment of C–H bonds.[74-75] In this paper, the application is made to C–H···N≡C– non-classical hydrogen bonding. Clear evidence for this interaction as a 'building block' in crystal engineering has been obtained from a large, statistical, survey of the CSD.[76] Accurate placement of C-H atoms in hydrocarbons will remove the E–H bond "normalizations" that are now routinely applied to compare experiment with computation in the analysis of H-bonding.[77] Meanwhile, Wood *et al.* have analyzed the CSD for dipolar C≡N···C≡N interactions in structures of organic nitriles, in view of the high polarity of these functional groups.[78] They found that some 37 % of structures containing nitriles met their rigorous search criteria for such interactions. We end this paper with a brief consideration of such nitrile-nitrile interactions, in conjunction with CH to nitrile H-bonding, as they have been encountered in the structures reported here.

## RESULTS AND DISCUSSION

### Chemical Background

**$C_{12}H_9CN$ valence isomers and related species**. Bromobenzobarrelene **1** (Scheme 1) is prepared by the reaction of benzyne with bromobenzene. This then undergoes nucleophilic substitution by CuCN, converting to the cyanobenzobarrelene, **2**.[49] Treatment with diazene (generated by acidification of potassium azodicarboxylate) selectively hydrogenates the unsubstituted stave of the barrelene, resulting in **3**.[10] Photolysis of **2** is carried out in a Pyrex vessel with a medium pressure mercury lamp, producing a mixture of valence isomers, **4**, **5**, and **6.**[49] Irradiation of **4** at 276 nm leads to 6-cyanobenzocyclooctatetraene (for which a crystal structure has not been determined), whose subsequent

isolation followed by further irradiation through a Pyrex filter (> 310 nm) leads to **7**.[46, 48] Irradiation of 7-cyanobenzocyclooctatetraene **5** at wavelengths ≥ 340nm, produces **8**.[47]

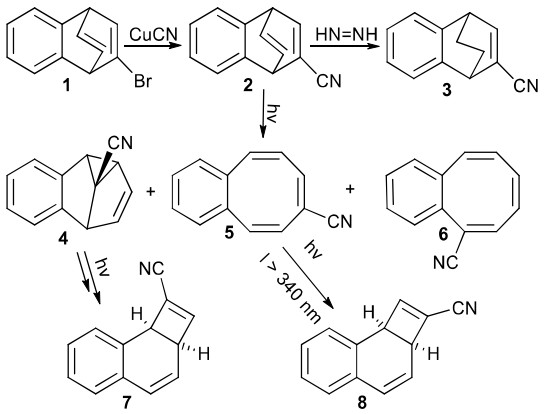


**Scheme 1**. Chemical and photochemical interconversion of $C_{12}H_9CN$ valence isomers and related species

**$C_{12}H_{11}CN$ valence isomers**. Compounds **9** and **10** are saturated analogs of **7** and **8,** and are produced in a 13:1 ratio by 313 nm irradiation of naphthalene in the presence of acrylonitrile (Scheme 2).[79] Numerous solvents were assessed in this synthesis, of which 2-propanol exhibited best overall quantum yield and lowest fraction of substituted naphthalene side products.

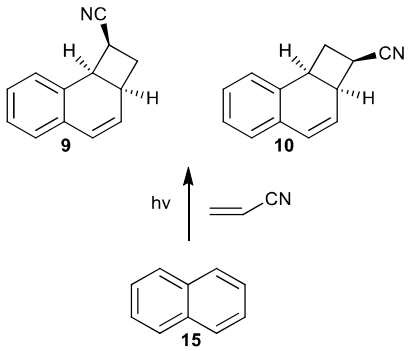


**Scheme 2**. Photochemical synthesis of $C_{12}H_{11}CN$ valence isomers

**$C_{12}H_8(CN)_2$ valence isomers**. Analogously to Scheme 1, dibromobenzobarrelene **16**, made from the dehydrobromination of higher brominated barrelenes such as tetrabromo-1,4-ethanonaphthalene,[9] reacts with CuCN to form the dinitrile **17**, which is then photolyzed with 254 nm radiation to produce a mixture of **11**, **12**, and **18** (82%, 6%, and 12%, respectively),[9, 80] which were separated by column chromatography (Scheme 3).

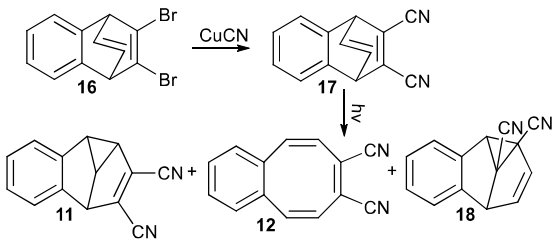


**Scheme 3**. Synthesis and photochemical interconversion of $C_{12}H_8(CN)_2$ valence isomers

Like the reactions described above, the cyanonaphthobarrelene **19** is obtained from the treatment of the corresponding bromonaphthobarrelene with CuCN; the latter barrelene is prepared as usual from the reaction of 2,3-naphthyne with bromobenzene.[49] Direct irradiation of **19** with 313 nm light produces a mixture of compounds **13**, **14**, and **20** in much the same way as the benzo-fused analogs **4** and **5** (Scheme 4).[50]

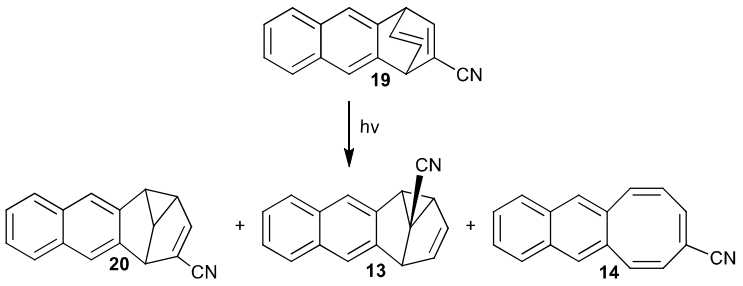


**Scheme 4**. Photochemical interconversion of $C_{16}H_{11}CN$ valence isomers

**Crystallography**

The new single-crystal X-ray diffraction structures obtained in this work belong to four major structural categories: benzobarrelenes (**1, 2**) and a partially hydrogenated analog **3**, benzo- and naphthosemibullvalenes (**4, 11, 13**), benzocyclooctatetraenes (**5, 6, 12, 14**), and di/tetra-hydrocyclobuta[*a*]naphthalenes (DCBN, TCBN) (**7, 8, 9, 10**). Because of the proclivity of photochemistry to produce many isomers via excited-state reactions, spread across all four categories are valence isomers with the formula $C_{13}H_9N$ (**2, 4, 5, 6, 7, 8**); two (**11**, **12**) are valence isomers of $C_{14}H_8N_2$ and two (**13**, **14**) are naphtho- rather than benzofused analogues of formula $C_{17}H_{11}N$.

**Barrelenes and a barrelene derivative**. The barrelenes in this series are typified by a benzo-fused bicyclic ring system with apical $sp^3$ carbons connected through two ethene staves. Our work includes the structure (Figure 1) of 2-bromo-1,4-dihydro-1,4-ethenonaphthalene, **1**, and 2-cyano-1,4-dihydro-1,4-ethenonaphthalene, **2**, both in non-centrosymmetric space groups ($Pca2_1$ and $P2_1$) and a derivative of **2** with one saturated and one unsaturated stave, 2-cyano-1,4-dihydro-1,4-ethanonaphthalene, **3**. Compounds **1** and **2** (Figure 1) have highly similar structures, excepting of course the substitution of Br (**1**) by the nitrile (**2**). In structure **3** in $P2_1/c$, there are two independent molecules in the asymmetric unit ($Z'$ = 2). One of these molecules is disordered (0.63/0.37) over the barrelene cage and nitrile substitution sites. A satisfactory disorder model was implemented, but the geometry reported for **3** is that of the ordered molecule since the disorder model accentuates a structural distortion that is not fully resolved. The geometry of **3** is distinct from **1** and **2**, owing to the hydrogenation of the unsubstituted ethene arm. When compared to the benzobarrelenes, as expected the C9-C10 bond is elongated to 1.5447(7) Å from 1.3250(19) in **2.** This also shortens the bonds to the apical $sp^3$ carbons from the substituted stave (C1-C2, C3-C4), and lengthens the bonds from the apical carbons to the unsubstituted stave (C1-C10, C4-C9) – see Table 1.

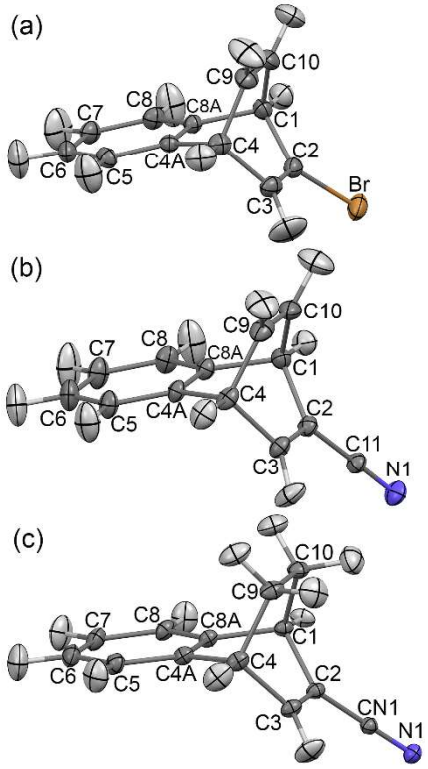


**Figure 1.** Displacement ellipsoid plots (50% probability) for structures at 173(2) K: (a) **1** (inverted), (b) **2,** and at 100(1) K: (c) **3**. The second (disordered) molecule in the asymmetric unit of **3** is omitted.

The geometries of **1** and **2** were compared to analogous barrelenes previously deposited to the CSD (Table 1), restricted to structures which are not part of a coordination complex and where the bicyclic barrelene moiety is not embedded in other rings (since additional ring strain could influence the geometries). Similar search criteria were used for compound **3**, save only that the search was for barrelenes with one saturated and one unsaturated stave. Individual bond lengths and angles were compared between our acquired structures and CSD analogs [8] using the 99% confidence interval (only deviations of more than s.u.×2.58 to the mean comparator values are taken to be significant).[81] By this method, compound **2** had one bond length (C3-C4) outside of the range of the analogs. However, when comparing the global average of bonds to the apical $sp^3$ carbons, the C3-C4 bond of **2** falls within the range and is not considered an outlier. Compound **1** has overall more short bonds than long (67%) and slightly more wider angles than narrower (58%) when compared to the average values for the analogous set of compounds, while compound **2** has overall more shorter bonds than longer (78%), and an equal number of angles wider and narrower than the mean. In view of the paucity of extant structures, wherever values from our new structures fit at the 99% confidence level, the means have been recomputed to include the results from this work (as indicated in footnotes to Tables 1-4).

Comparing **3** to analogous structures from the CSD is not such a straightforward task, as the set of 18 unique comparators (some of which have up to 6 independent barrelene moieties, for a total of 39 comparative geometries) are deeply affected by disorder, with only 4 unique comparators encompassing 8 total entries judged by us as free of disorder. Goh et al.[6] analyze this issue in detail, and suggests that the disorder in these mixed ene/ane barrelene cages is due to a high similarity in crystal-packing requirements of the $H_2C$-$CH_2$ and the HC=CH staves. Uno[82] and Mithani[14] specifically mention this disorder,

but do not address it at any length, while Aotake,[12] Tanaka,[13] and Kaya[5] do not mention any ene/ane disorder in the barrelene cages. Unsurprisingly, the C-C bonds of these staves, C2-C3 and C9-C10, experience the greatest distortion of the disorder. From the CSD comparators without disorder, the average length of C9-C10 ($H_2C$-$CH_2$) is 1.54(2) Å, and C2-C3 (HC=CH) is 1.316(10) Å, which is within the normal range for single and double C-C bonds, and is the motif that we must necessarily expect for these ordered structures. In the disordered structures, the average bond lengths of C9-C10 and C2-C3 are 1.46(2) Å and 1.40(2) Å respectively, intermediate between single and double bonds. These data can be found in full in Table S20 in the SI.

**Table 1**. Selected bond distances and angles in structures of the barrelenes and barrelene derivatives.[a]

| **Bonds (Å)** | **1** | **2** | **Average[b]** | **3[c]** | **Average[d]** |
|---|---|---|---|---|---|
| **C1-C2** | 1.5242(19) | 1.5240(15) | 1.534 (8) | 1.5178(6) | 1.513(12) |
| **C1-C8A** | 1.5256(16) | 1.5188(15) | 1.530 (14) | 1.5132(7) | 1.516(16) |
| **C1-C10** | 1.533(2) | 1.5181(16) | 1.529(7) | 1.5630(7) | 1.558(9) |
| **C2-C3** | 1.3336(19) | 1.3306(16) | 1.324(7) | 1.3480(7)[e] | 1.316(10) |
| **C3-C4** | 1.528(2) | 1.5131(15) | 1.531(10) | 1.5064(7) | 1.513(9) |
| **C4-C4A** | 1.5269(18) | 1.5196(15) | 1.537(14) | 1.5115(7) | 1.512(5) |
| **C4-C9** | 1.531(2) | 1.5190(17) | 1.531(9) | 1.5652(7) | 1.558(12) |
| **C4A-C8A** | 1.3965(17) | 1.3879(13) | 1.405(13) | 1.4009(6) | 1.394(5) |
| **C9-C10** | 1.327(2) | 1.3250(19) | 1.322(10) | 1.5447(7) | 1.54(2) |
| **Angles (°)** | | | | | |
| **C1-C2-C3** | 115.13(13) | 114.45(9) | 113.6 (15) | 114.77(4) | 114.5(5) |
| **C1-C8A-C4A** | 112.05(11) | 112.73(9) | 112.5 (8) | 112.97(4) | 113.0(6) |
| **C1-C10-C9** | 113.30(13) | 113.98(12) | 113.7 (12) | 109.32(4) | 109.3(8) |
| **C2-C1-C10** | 105.56(11) | 105.44(9) | 106.5(11) | 105.43(4) | 105.5(5) |
| **C2-C1-C8A** | 105.43(11) | 104.28(9) | 104.8(9) | 107.52(4) | 108.1(6) |
| **C2-C3-C4** | 111.88(13) | 113.01(11) | 114.0(15) | 113.66(4)[e] | 114.7(5) |
| **C3-C4-C9** | 106.63(12) | 106.41(10) | 106.5(8) | 105.43(4) | 105.8(9) |
| **C3-C4-C4A** | 105.76(11) | 104.59(9) | 104.7(6) | 108.12(4) | 108.2(7) |
| **C4A-C4-C9** | 105.14(11) | 105.72(10) | 104.8(12) | 106.35(4) | 105.1(7) |
| **C4-C4A-C8A** | 112.38(11) | 112.35(10) | 111.8(10) | 113.26(4) | 113.0(6) |
| **C4-C9-C10** | 113.78(13) | 113.70(10) | 114.1(13) | 109.53(4) | 109.6(8) |
| **C8A-C1-C10** | 105.21(11) | 105.33(9) | 105.0(8) | 106.13(4) | 105.7(7) |

[a] Atom labels are taken from the first exemplar (see Fig. 1a) and applied to all structures for ease of comparison. The atom numbering schemes should be consulted for identifying specific entries. Errors for individual structures are s.u.; errors for averages are std. dev. of the sets of values.

[b] Average of specified bond length/angle of structural analogs collected from the CSD. Values from structures introduced in this paper are included in this average unless otherwise specified. Comparators used in this category: FIBDAX,[3] FIBDEB,[3] FIBDOL,[3] FIXLIJ,[4] GEGGEE,[83] LEKLAO,[18] LEZLOR,[17] LICGIP,[3] LICGOV,[3] LICGUB,[3] LICHAI,[3] LICHEM,[3] MEYHOP,[9] SATPUY,[84] TUGHAH,[2] TUGHEL,[2] WEJBOC,[85] XAHFAR,[1] XAHFEV[1]

[c] Geometry of the disordered molecule in the asymmetric unit is omitted.

[d] Average of specified bond length/angle of structural analogs collected from the CSD. Values from structures introduced in this paper are included in this average unless otherwise specified. Comparators used in this category: NAHZAX,[11] TIVFUZ,[86] VAKBAK,[87] ZIZZOX.[88] Comparators which were obtained from the CSD, but excluded due to disorder: FALHIK,[89] MICBUW,[6] MICCAD,[6] MICCEH,[6] OCOHUL,[82] PIBCIO,[13] PIBCOU,[13] PIBCUA,[13] PIBDAH,[13] PIBDEL,[13] PIBDUB,[13] RAKPUQ,[5] WEXRIA,[14] YOSFAP,[12]

[e] Statistical outlier omitted from the averaged values

The structure of compound **3** conforms closely to the *reliable* comparator structures in the CSD, with all but one bond length and all but one bond angle fitting within the range of the analog values at the 99% confidence level, and with deviations from the mean tending towards more longer bonds than shorter (67%), and slightly more narrower angles than wider (58%). The Cremer-Pople puckering parameters,[90-92] hereafter referred to as puckering parameters, for the barrelene moieties of **1** – **3** (Table S1) all closely conform to boat geometry (Q = 0.7529 – 0.8487, $\theta \approx \pi/2$, $\phi \approx \pi$), consistent with the absence of steric effects in this substitution pattern (contrast a previously reported tetrabromobarrelene). [9]

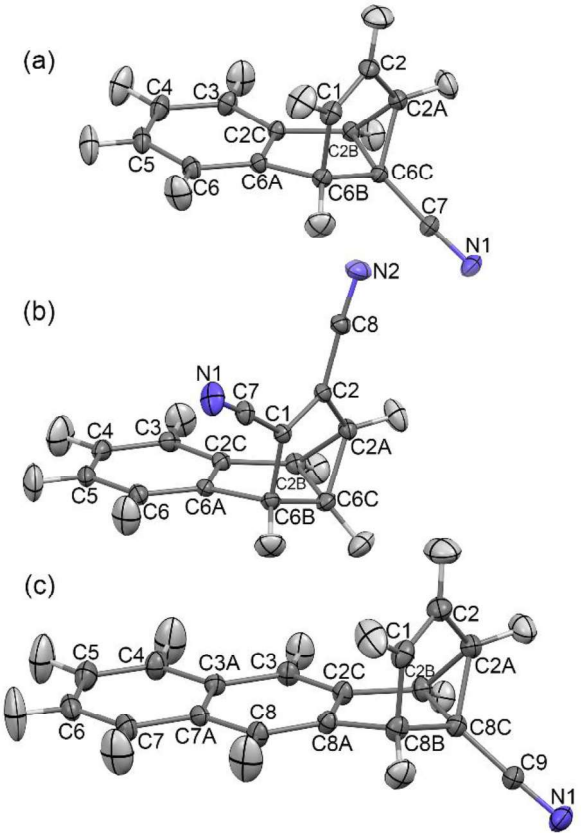


**Figure 2.** Displacement ellipsoid plots (50% probability) for structures at 173(2) K: (a) **4** (inverted) (b) **11** (a second molecule in the asymmetric unit is highly similar and is omitted), and (c) **13**.

**Benzo- and naphthosemibullvalenes**. Semibullvalenes have a characteristic three-ring system consisting of two fused 5-membered rings which are bridged (at C2A/C2B) to form a 3-membered ring (Figure 2). In our compounds **4**, **11**, and **13**, one of the 5-membered rings is also fused to a benzene ring along the C2C-C6A position, and the other 5-membered ring has a formal double bond along C1-C2. 2*a*,2*b*,6*b*,6*c*-tetrahydrobenzo(*a*)cyclopropa(*ca*)pentalene-6C-carbonitrile, **4**, crystallizes in $P2_12_12_1$ with $Z' = 1$ and bears the nitrile substituent at the central apical $sp^3$ site C6C. In dinitrile variant 2*a*,2*b*,6*b*,6*c*-tetrahydrobenzo(*a*)cyclopropa(*ca*)pentalene-1,2-dicarbonitrile, **11** (Pbca, $Z' = 2$), the cyano groups are located on $sp^2$ C atoms of the cage edge rather than the apical $sp^3$. It crystallizes with two ordered molecules in the asymmetric unit which have very similar geometries, dimensions of which are presented

comparatively in Table 2 (as **11**[1] and **11**[2]); only one is shown in Figure 2b. The C1-C2 type bond lengths of **11**, at 1.3520(12) and 1.3506(12) Å, are anomalously long due to the two nitrile substituents at these C atoms on either side of a formal double bond, for which these data are excluded from the average comparator distances from the CSD. The C6A-C6B bond length in **4** is sufficiently short as to make it an outlier, and it has therefore been excluded from the combined average. 2a,2b,8b,8c-tetrahydro-cyclopropa[3,4]pentaleno[1,2-b]naphthalene-8C-carbonitrile, **13** ($P2_12_12_1$ with $Z'$ = 1, Fig. 2c) is a direct naphtho-fused analog to **4** and one of two exemplars in this study with the extended annulene. It is the first structure of its kind to be reported.

**Table 2**. Selected bond distances and angles in structures of the benzo- and naphthosemibullvalenes.

| **Bonds (Å)** | **4** | **11**[1] | **11**[2] | **13**[a] | **Average**[b] |
|---|---|---|---|---|---|
| C1-C2 | 1.3311(5) | 1.3520(12)[c] | 1.3506(12)[c] | 1.326(3) | 1.327(7) |
| C1-C6B | 1.5171(5) | 1.5286(13) | 1.5214(13) | 1.524(3) | 1.522(15) |
| C2-C2A | 1.4706(4) | 1.4754(13) | 1.4732(13) | 1.470(3) | 1.478(7) |
| C2A-C2B | 1.5452(4) | 1.5757(14) | 1.5743(14) | 1.538(3) | 1.566(25) |
| C2A-C6C | 1.5102(4) | 1.5020(14) | 1.5050(15) | 1.515(3) | 1.510(12) |
| C2B-C2C | 1.4727(4) | 1.4792(13) | 1.4735(13) | 1.474(3) | 1.481(6) |
| C2B-C6C | 1.5107(4) | 1.5021(14) | 1.5003(15) | 1.511(3) | 1.508(14) |
| C2C-C6A | 1.3939(4) | 1.4050(13) | 1.4017(12) | 1.416(3) | 1.408(13) |
| C6A-C6B | 1.5129(4)[c] | 1.5191(13) | 1.5221(14) | 1.517(3) | 1.526(6) |
| C6B-C6C | 1.5424(4) | 1.5473(14) | 1.5513(15) | 1.542(3) | 1.553(15) |
| **Angles (°)** | | | | | |
| C1-C2-C2A | 111.72(3) | 111.18(9) | 111.15(9) | 111.15(9) | 111.5(9) |
| C1-C6B-C6A | 101.31(2) | 101.90(7) | 101.93(7) | 101.93(7) | 102.0(12) |
| C1-C6B-C6C | 102.72(2) | 102.85(8) | 102.77(9) | 102.77(9) | 103.2(6) |
| C2-C2A-C2B | 120.72(3) | 120.01(9) | 120.70(9) | 120.70(9) | 120.5(9) |
| C2-C1-C6B | 110.82(3) | 110.54(9) | 110.42(9) | 110.42(9) | 110.7(9) |
| C2-C2A-C6C | 105.81(3) | 106.56(9) | 106.56(9) | 106.56(9) | 106.6(10) |
| C2A-C2B-C2C | 119.96(3) | 122.26(9) | 121.17(9) | 121.17(9) | 120.7(14) |
| C2A-C2B-C6C | 59.22(2) | 58.39(6) | 58.55(7) | 58.55(7) | 58.8(10) |
| C2A-C6C-C2B | 61.53(2) | 63.27(7) | 63.18(7) | 63.18(7) | 62.5(15) |
| C2A-C6C-C6B | 104.92(2) | 105.38(9) | 104.77(9) | 104.77(9) | 104.2(8) |
| C2B-C2A-C6C | 59.253(19) | 58.37(7) | 58.26(7) | 58.26(7) | 58.7(9) |
| C2B-C2C-C6A | 110.84(3) | 110.05(9) | 110.35(9) | 110.35(9) | 110.3(7) |
| C2B-C6C-C6B | 105.74(2) | 104.96(9) | 104.86(9) | 104.86(9) | 105.2(7) |
| C2C-C2B-C6C | 106.05(2) | 107.23(9) | 107.59(9) | 107.59(9) | 106.9(8) |
| C2C-C6A-C6B | 109.59(2) | 109.16(8) | 109.15(9) | 109.15(9) | 109.2(6) |
| C6A-C6B-C6C | 103.19(2) | 103.84(8) | 104.05(9) | 104.05(9) | 103.3(4) |

[a] Atom labels are taken from the first exemplar (see Fig. 2a) and applied to all structures for ease of comparison. The atom numbering schemes should be consulted for identifying specific entries. Errors for individual structures are s.u.; errors for averages are std. dev. of the sets of values.

[b] Average of specified bond length/angle of structural analogs collected from the CSD. Values from structures introduced in this paper are included in this average unless otherwise specified. Comparators used in this category: CEFPOU,[16] FOYGEF,[20] FOYGUV,[20] FOYHAC,[20] LEKLES,[18] LEKLIW,[19] LEZLUX,[17] RUNZIK,[21] SAGSEZ,[22] SUFTIY.[15]

[c] Statistical outlier omitted from the averaged values.

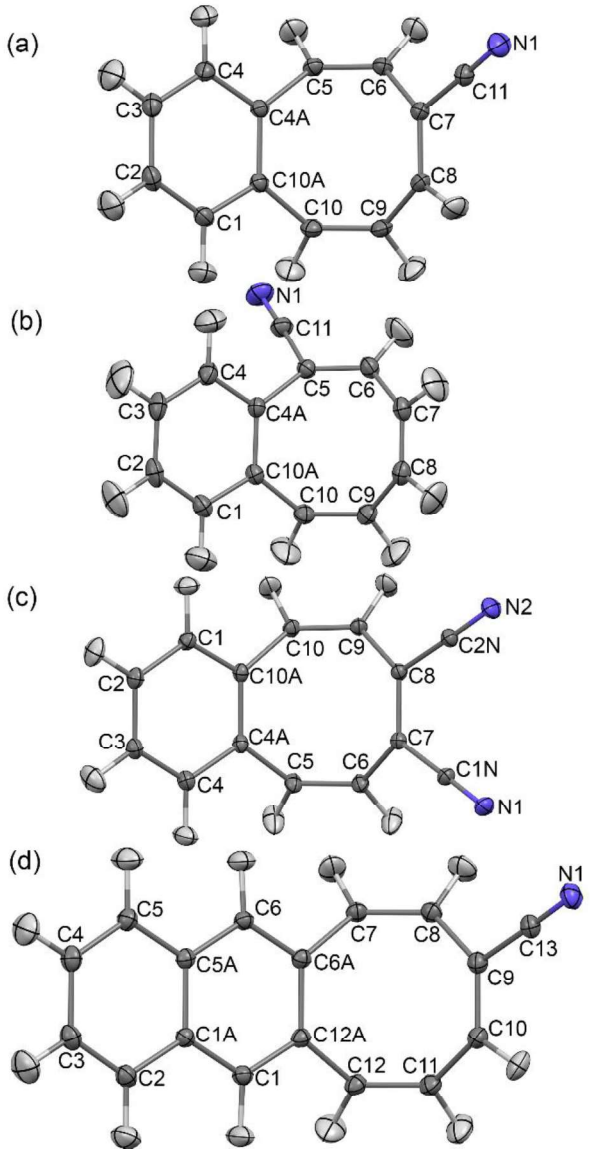


**Figure 3.** Displacement ellipsoid plots (50% probability) for structures at 173(2) K: (a) **5**, (b) **6**, and at 100(1) K: (c) **12** (second molecule in asym. unit omitted) and (d) **14** (enantiomer of asym. unit; major comp. of nitrile disorder shown).

A search for analogs in the CSD was restricted to benzosemibullvalenes which are not coordinated to a metal and excluded substructures in which the semibullvalene skeleton atoms are embedded in other rings. There are no naphtho-fused semibullvalenes in the CSD, so the geometry of **13** is compared to the same benzo-fused structures as compounds **4** and **11**. The benzo-fused analogue bond lengths and angles in compound **4** have more shorter bonds than longer (70%), and slightly more wider angles than narrower (56%). $\mathbf{11^1}$ and $\mathbf{11^2}$ have more shorter than longer bonds (70% and 80%, respectively), $\mathbf{11^1}$ has more narrow angles than wide (62%), and $\mathbf{11^2}$ has equal numbers of short and wide angles (50%). Bond lengths and angles for naphtho-fused **13** all fall within the range of the CSD comparators at the 99% confidence level and are thus included in the combined average values presented below. There are slightly more short

bonds than long (60%), and equal numbers of narrow and wide angles (50%). The puckering parameters[90-92] of the 5-membered rings in compounds **4**, **11**, and **13** (Table S2) are all consistent with twist ring conformations ($q_2$ = 0.1844 – 0.225, $\phi_2 \approx \pi/5$ +18°). The 7-membered rings of these compounds (C1-C2-C2A-C2B-C2C-C6A-C6B in compounds **4** and **11**, for example) are all in a twist-boat conformation ($q_2$ 1.1575 – 1.164, $\phi_2 \approx \pi/14$, $q_3$ = 0.192 – 0.2004, $\phi_3 \approx \pi/14$).

**Benzo- and naphthocyclooctatetraenes**. Benzo-fused 7-benzocyclooctenecarbonitrile **5** crystallizes in the non-centrosymmetric Sohncke space group ($P2_12_12_1$ with $Z'$ = 1), whereas the remaining three exemplars crystallize centrosymetrically. Structure **6** is isomeric 5-benzocyclooctenecarbonitrile ($P\bar{1}$, $Z'$ = 1); **12**, is 8-benzocyclooctenedicarbonitrile ($P2_1/c$, $Z'$ = 2; only the first exemplar of these highly similar structures is shown in Figure 3c) while **14** is naphtho-fused 9-cycloocta[1,2-*b*]naphthalenecarbonitrile ($P2_1/c$, $Z'$ = 1). The placement of the nitrile substituent in **14** was found to be disordered (0.80/0.20) between attachment to C9 and C10, respectively. An excellent two-part disorder model was refined and the reported geometry of **14** is from the major component only. As with other searches in this work for comparators in the CSD, those coordinated to metals or embedded in other rings were excluded. There are no naphtho-fused COTs in the CSD, so the geometry of **14** is compared to the same benzo-fused COT structures as compounds **5**, **6**, and **12**.

**Table 3**. Selected bond distances and angles in structures of the benzo- and naphthocyclooctatetraenes.[a]

| **Bonds (Å)** | **5** | **6** | **12[1]** | **12[2]** | **14**[b] | **Average**[c] |
|---|---|---|---|---|---|---|
| C4A-C5 | 1.4736(9) | 1.4821(4) | 1.4760(10) | 1.4826(11) | 1.4803(8) | 1.480(6) |
| C4A-C10A | 1.3970(9) | 1.3916(4) | 1.4002(10) | 1.4018(10) | 1.4266(8)[d] | 1.400(11) |
| C5-C6 | 1.3298(9) | 1.3383(4) | 1.3387(11) | 1.3377(11) | 1.3408(9) | 1.331(7) |
| C6-C7 | 1.4686(9) | 1.4536(4) | 1.4717(10) | 1.4721(10) | 1.4681(9) | 1.467(10) |
| C7-C8 | 1.3421(9) | 1.3334(4) | 1.3570(10)[d] | 1.3546(10)[d] | 1.3496(9) | 1.33(2) |
| C8-C9 | 1.4551(9) | 1.4549(4) | 1.4696(10) | 1.4739(11) | 1.4604(9) | 1.466(10) |
| C9-C10 | 1.3334(10) | 1.3334(4) | 1.3391(11) | 1.3401(11) | 1.3408(9) | 1.333(9) |
| C10-C10A | 1.4733(9) | 1.4678(4)[d] | 1.4820(10) | 1.4791(10) | 1.4809(8) | 1.483(8) |
| **Angles (°)** | | | | | | |
| C10-C10A-C4A | 123.90(6) | 124.02(2) | 124.05(7) | 123.15(7) | 124.33(5)[d] | 123.0(10) |
| C4A-C5-C6 | 126.62(6) | 126.95(3) | 127.90(7) | 127.44(7) | 128.60(6) | 127.1(18) |
| C10A-C4A-C5 | 123.94(6) | 122.33(2) | 124.08(7) | 123.86(7) | 124.11(5) | 123.0(15) |
| C5-C6-C7 | 125.54(6) | 125.05(3) | 127.82(7) | 126.27(8) | 127.32(6) | 125.8(17) |
| C6-C7-C8 | 126.25(6) | 124.83(3) | 126.35(7) | 125.21(7) | 126.69(6) | 126(2) |
| C7-C8-C9 | 125.59(6) | 126.99(3) | 126.07(7) | 125.60(7) | 126.33(7) | 125.6(15) |
| C8-C9-C10 | 126.48(6) | 127.61(3) | 127.16(7) | 126.08(7) | 127.75(6) | 126.3(19) |
| C9-C10-C10A | 126.72(6) | 126.58(3) | 128.25(7) | 127.49(8) | 128.84(6)[d] | 126.9(18) |

[a] Atom labels are taken from the first exemplar (see Fig. 3a) and applied to all structures for ease of comparison. The atoms numbering schemes should be consulted for identifying specific entries. Errors for individual structures are s.u.; errors for averages are std. dev. of the sets of values.

[b] Disorder in the nitrile position; the major component of the two-part disorder model is reported here.

[c] Average of specified bond length/angle of structural analogs collected from the CSD. Values from structures introduced in this paper are included in this average unless otherwise specified. Comparators used in this category: BUYYUP,[93] CUDYUV,[94] FIVHIB,[95] LEZMAE,[17] LIPVAJ,[96] QOGYER,[97] QOGZAO,[82] OWUVUA,[32] OWUWAH,[32] OWUWEL.[32]

[d] Statistical outlier omitted from the averaged values.

As in the similar situation in compound **11**, the C7-C8 double bond of **12** is significantly lengthened compared to the other double bonds due to the substituent effects of the nitriles at either end of the double bond. In a search of the CSD, 32 structures were located with *cis*-1,2-dicyanoethenes that are also attached to two $sp^3$ carbon atoms, yielding a mean C=C bond length of 1.341 (6) Å. In 1,996 cases of analogous *cis*-1,2-ethenes with hydrogen substituents in place of the cyano groups, the average was found to be 1.31 (5) Å, indicative of significant lengthening caused by the two flanking nitriles. Naturally, the C7-C8 bond lengths of $\mathbf{12^1}$ and $\mathbf{12^2}$ are excluded from the combined average for BCOT and NCOT double bonds presented in Table 3. This elongated C7-C8 bond widens several angles around the COT ring, resulting in the exclusion of the C5-C6-C7 angle of $\mathbf{12^1}$ from the combined average.

The ring fusion C6A-C12A bond in compound **14** (i.e. C4A-C10A entry in Table 3) is anomalously long compared to other collected structures. This is thought to be due to the polycyclic system sacrificing the aromaticity of the ring to which the COT is fused in order to enhance the aromaticity of the remote ring in accordance with Clar's rule (i.e. favouring the Kekulé resonance structure with the greatest number of aromatic π-sextets).[98] This effect also influences the bond angles in the COT ring which results in the exclusion of the C10-C10A-C4A and C9-C10-C10A angles from the combined average. The bond lengths and angles of compound **5** all fit into the range of the analogous structures collected from the CSD, with equal numbers of longer bonds than shorter (50%), and predominantly wider angles than narrower (75%). Compound **6** has a long C10-C10A bond which is excluded from the combined average, but otherwise its bond lengths and angles fit within the range of analogs with equal numbers of longer than shorter bonds (50%), and equal numbers of narrower and wider angles (50%) when compared to means. The two independent molecules of compound **12**, the dinitrile, have highly similar structures where the bond lengths tend to be longer than the average (75% and 88% for $\mathbf{12^1}$ and $\mathbf{12^2}$, respectively), and bond angles are mostly wider than narrower (100% and 88%). Compound **14** has more longer than shorter bonds compared to the average (75%), and all bond angles examined are wider than the average (100%). The puckering parameters[90-92] for the 8-membered rings in **5**, **6**, **12**, and **14** (Table S3) are found to be consistent with tub geometry ($q_2$ = 1.1272 – 1.1821, $\phi_2 \approx \pi/4$, $q_3$ = 0.0134 – 0.0468, $q_4$ = -0.0032 – 0.0107), which is strongly conserved with some minor twisting, which, however, does not seem to fit a clear pattern for number and locations of the substituents. We can presume that the rigid benzo-fusing at one of the two edges should be effective at sustaining the tub shape.

**DCBN and TCBN derivatives**. Compounds **7 – 10** are polycyclic systems in which a (ring-fused) 1,3-dicyclohexene ring is fused to a cyclobutane or cyclobutene ring at the saturated carbons. In 1-2*a*,8*b*-dihydrocyclobuta[*a*]naphthalenecarbonitrile, **7**, ($P2_1/n$, $Z'$ = 1) and in 2-2*a*,8*b*-dihydrocyclobuta[*a*] naphthalenecarbonitrile, **8** ($P2_1/c$, $Z'$ = 1), it is a cyclobutene ring (Figure 4a,b). The benzene ring fusion is at C4A-C8A, and cyclobutene ring is at C2A-C8B. Since the two nitrile substituents occur at the ethene bridge atoms (C1,2) steric congestion that might perturb the basic structure is not expected and, consequently, the base six-membered ring in **7** is found to be close to planarity (maximum deviation from the L.S. plane is 0.020(1) Å) and the cyclobutene is quite planar (deviation of only 0.001(1) Å). The 'envelope fold angle' between these L.S. planes is 65.62(3)°. In **8**, the two rings have deviations of 0.018(1) and 0.045(1) Å and the 'envelope' dihedral is 65.35(2)°.

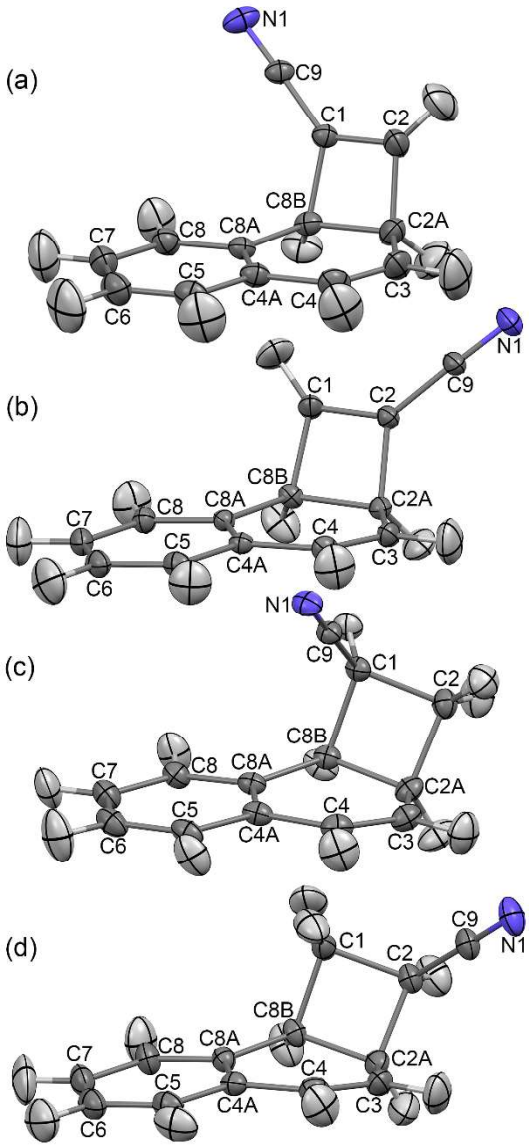


**Figure 4.** Displacement ellipsoid plots (50% probability) for structures at 173(2) K: (a) **7**, (b) **8**, and (d) **10**, and at 100(1) K: (c) **9** (inverted).

In *endo*-1-*1*,2,2*a*,8*b*-tetrahydrocyclobuta[*a*]naphthalenecarbonitrile, **9** ($P2_12_12_1$, $Z'$ = 1) and *endo*-2-1,2,2*a*,8*b*-tetrahydrocyclobuta[*a*]naphthalenecarbonitrile, **10** ($P2_1/n$, $Z'$ = 1), both of the nitrile substituents are oriented in towards the fold created by the ring fusions (Fig 4c,d). In these structures, the saturation of the C1–C2 bond induces considerable conformational changes. Thus, in **9** the maximum deviations from L.S. planes for the 4- and 6-membered rings (fused benzo-rings are omitted from this analysis) are 0.106(1) and 0.128(1) Å, respectively. In **10**, these values are 0.135(1) and 0.153(1) Å. Interestingly, despite the considerable ring twisting, the 'envelope' dihedral angles between these L.S. average planes remain quite similar to the unsaturated analogs. The angles for **9** and **10** are 66.36(7) and 67.81(7), respectively, and thus very slightly less acute than in **7** and **8**.

**Table 4**. Selected bond distances and angles in structures of the DCBN and TCBN derivatives.

| **Bonds (Å)** | **7** | **8** | **DCBN Ave** [a] | **9** | **10** | **TCBN Ave** [b] |
|---|---|---|---|---|---|---|
| C1-C2 | 1.3393(5) | 1.3438(4) | 1.340(4) | 1.5571(13) | 1.5422(14) | 1.542(18) |
| C1-C8B | 1.5239(5) | 1.5178(4) | 1.522(12) | 1.5773(12) | 1.5414(14) | 1.57(3) |
| C2-C2A | 1.5216(6)[c] | 1.5283(4) | 1.527(4) | 1.5547(15) | 1.5528(14) | 1.562(15) |
| C2A-C3 | 1.4942(6) | 1.4935(4) | 1.492(12) | 1.4954(16) | 1.4805(14) | 1.48(2) |
| C2A-C8B | 1.5742(6) | 1.5753(4) | 1.579(6) | 1.5571(13) | 1.5399(13) | 1.56(2) |
| C3-C4 | 1.3373(6) | 1.3397(4)[c] | 1.334(6) | 1.3456(16) | 1.3315(14) | 1.324(17) |
| C4-C4A | 1.4623(6) | 1.4642(4) | 1.462(8) | 1.4678(14) | 1.4557(13) | 1.467(18) |
| C4A-C8A | 1.4042(5) | 1.4029(4) | 1.405(6) | 1.4048(14) | 1.3928(12) | 1.41(3) |
| C8A-C8B | 1.5011(5) | 1.5019(4) | 1.507(7) | 1.4993(13) | 1.4865(13) | 1.51(3) |
| **Angles (°)** | | | | | | |
| C1-C2-C2A | 93.64(3) | 94.68(2) | 94.4(8) | 89.48(7) | 88.07(8) | 88.8(12) |
| C1-C8B-C2A | 84.83(3) | 86.30(2) | 85.6(8) | 88.66(7) | 88.56(7) | 87.7(14) |
| C1-C8B-C8A | 114.49(3) | 116.67(3)[c] | 113.9(15) | 117.87(8) | 117.58(9) | 116.2(18) |
| C2-C1-C8B | 95.21(3) | 93.97(3) | 94.5(8) | 88.46(7) | 88.40(8) | 89.1(12) |
| C2-C2A-C3 | 115.07(4) | 114.18(3) | 115.4(13) | 113.25(10) | 113.17(9) | 117(3) |
| C2-C2A-C8B | 86.32(3) | 84.93(2) | 85.3(9) | 89.28(7) | 88.07(7) | 88.8(8) |
| C2A-C3-C4 | 122.27(4) | 122.78(3) | 121.6(17) | 122.97(10) | 122.71(10) | 123.2(16) |
| C2A-C8B-C8A | 117.10(3) | 117.61(2)[c] | 115.5(10) | 118.39(8) | 117.45(9) | 116(3) |
| C3-C2A-C8B | 115.97(3) | 115.18(3)[c] | 117.0(12) | 113.23(9) | 113.19(9) | 114(2) |
| C3-C4-C4A | 123.39(4) | 123.20(3) | 123.6(5) | 122.94(10) | 122.81(10) | 123.0(16) |
| C4-C4A-C8A | 120.50(3) | 120.47(3) | 120.6(7) | 119.96(9) | 119.62(9) | 119.4(14) |
| C4A-C8A-C8B | 120.65(3) | 120.30(3) | 120.4(4) | 118.95(8) | 119.05(8) | 120.0(10) |

[a] Average of specified bond length/angle of structural analogs collected from the CSD. Values from structures introduced in this paper are included in this average unless otherwise specified. Comparators used in this category: DIWVUD,[99] MONPHC,[100] MONPHD.[100] Errors for individual structures are s.u.; errors for averages are std. dev. of the sets of values.

[b] Average of specified bond length/angle of structural analogs collected from the CSD. Values from structures introduced in this paper are included in this average unless otherwise specified. Comparators used in this category: AXOQIO,[41] EWIXUF02,[40] FMPCBN,[101] HZOBUR,[102] JUYYOR,[44] PHBNPH,[45] QETHAY,[43] QETHEC,[43] RECGAH,[103] YEQFIJ,[42] YICXOX[104].

[c] Statistical outlier omitted from the averaged values.

Separate comparator groups were sought from a search of the CSD for the DCBN and TCBN structure types (Table 4). It is notable that there are only 3 unique comparators in the CSD for DCBNs with the search filters adopted in this work, namely those entries which are coordinated to a metal or in which the skeleton of the DCBN are embedded in other rings have been excluded. The C2A-C8B-C8A angle in both **7** and **8** is significantly wider than the mean by 1.6° and 2.1°, respectively. Angles C1-C8B-C8A and C3-C2A-C8B in structure **8** also do not fit the average, and the C2-C2A bond length in **7** is anomalously short. Structures **7** and **8** have more shorter bonds than longer compared to means (67% for both), and more wider than narrower angles (67% and 58%). Structures **9** and **10** have more shorter bonds than longer compared to means (56% and 78%, respectively). There are equal numbers of wide and narrow angles in structure **9** (50%), and more narrower angles than wider in structure **10** (67%). Puckering parameters[90-92] for **9** indicate the 4-membered ring has puckered geometry ($q_2$ = -0.2094), and the 6-membered cyclohexyl ring adopts a conformation between envelope and half-chair, favouring envelope (q = 0.1628, θ = 61.0°,

ϕ = 310.7°). For **10**, the 4-membered ring is puckered ($q_2$ = -0.2678), and the 6-membered cyclohexyl ring is intermediate between envelope and twist-boat, slightly favouring envelope (q = 0.2504, θ = 115.4°, ϕ = 134.6°). Puckering parameters cannot be assigned for **7** and **8** due to τ values less than 5°, as expected for these highly planar rings. Puckering parameter data for **9** – **10** can be found in Table S4. A structure of **9** was claimed previously in 1968,[51] but as being in $P2_1/c$ (Z' = 1) and only a room-temperature unit cell was determined. It contains neither atom coordinates nor R-factor statistics, and as such no comparisons can be made.

**Structure Refinement with Aspherical Atomic Scattering Factors**.

HAR was undertaken for all 14 structures using the recently reported NoSpherA2 software.[56] This program is included with current releases of the Olex2 crystallographic software suite[105] and harmonizes with the olex2.refine engine.[55] It seamlessly integrates with several popular density-functional theory (DFT) computational packages, and here we have used it with the freely downloadable ORCA computational software suite.[106-107] Fast and accurate DFT functionals such as B3LYP or PBE enable the computation of accurate custom atom scattering factors that directly reflect the electron densities of all the atoms within their structural environment, and thus polarized correctly to their precise locations in the structures. This *quantum crystallography*[56, 60-61] approach remains a fully experimental structure determination because DFT is used to calculate atomic scattering factors, which are then used to construct the $F_{calc}$ values for the model and minimized against $F_{obs}$ in the conventional manner. The benefit comes, however, from the customization of the atom scattering factors, rather than using one set of standard compiled factors from very old self-consistent field (SCF) calculations on a set of spherical, neutral atoms.[108] For the fourteen structures reported in this work, comparison of the NoSpherA2 refinements with well-performed conventional models refined in the IAM, the structure accuracy as indicated by the average precision of the C–C bonds (as calculated by PLATON,[109-110] and prominently displayed near the tops of all CheckCIF reports) improved, on average, from 0.0019 to 0.0012 Å, a 42% improvement, as detailed in Table 5. Notably, *all* the structures gained in this precision indicator, ranging from 9 to 73% improvement; that is to say, none of the refinements deteriorated from the use of this HAR method.

Interestingly, and consistent with our previous experience applying HAR with NoSpherA2 on a series of organophosphine derivatives,[58] there is a strong trend in this *improvement* in heavy-atom bond precision (in both cases using the average C–C bond precision computed by PLATON,[109-110] as these are the most common in both sets of structures) with data/model quality. A correlation graph is included with the Supporting Information (Fig. S3), which shows high compliance for the more accurate data sets and greater scatter with lower data quality. We think that these results are important, first because of the evident improvement in accuracy of the whole structure (i.e. not just nice-looking ADPs for H-atoms) but secondly, for the incentive to chemists to strive for the best quality crystals possible and obtain the highest quality diffraction data.[111] With these modern HAR methods, it is now possible to exploit more of the information immanent in superior structure data. This certainly justifies the time and effort expended to implement HAR via NoSpherA2, to the point where it probably ought to become routine practice.[52-53] The improvement in the refinement model for the heavy atoms is expected with HAR in conjunction with higher resolution data; by contrast, as Kleemiss *et al.* have clearly shown, the major information in the atomic scattering factors for hydrogen is found at lower values of sinθ/λ.[56] Thus, accurate H-atom placement and ADP refinement is entirely feasible at IUCr diffraction limits (and with Cu data).[52] The major limitation for H-atom refinement is thus not resolution, but the increased numbers of parameters needing

refinement. Higher resolution – if the $I/\sigma(I)$ ratio remains sufficient – may provide the additional data required. Alternatively, the H-atoms could be positionally refined but with isotropic displacements.[58]

**Table 5.** Summary of Results and Quality Analysis for NoSpherA2 Refinement of Structures.[a,b]

| Structure | C-C bond precision in Å [c] | Deg. impr. | $R_1$ | $R_{int}$ | Data/par. ratio |
|---|---|---|---|---|---|
| **1** | 0.0019 – 0.0028 | 32.1% | 0.0181 | 0.0273 | 12.0 |
| **2** | 0.0016 – 0.0025 | 36.0% | 0.0270 | 0.0216 | 11.3 |
| **3** | 0.0007 – 0.0015 | 53.3% | 0.0168 | 0.0270 | 8.4 |
| **4** | 0.0004 – 0.0015 | 73.3% | 0.0092 | 0.0118 | 11.0 |
| **5** | 0.0009 – 0.0015 | 60.0% | 0.0199 | 0.0159 | 11.6 |
| **6** | 0.0005 – 0.0015 | 66.7% | 0.0120 | 0.0060 | 11.3 |
| **7** | 0.0006 – 0.0016 | 62.5% | 0.0143 | 0.0169 | 10.5 |
| **8** | 0.0005 – 0.0014 | 64.3% | 0.0121 | 0.0186 | 10.2 |
| **9** | 0.0015 – 0.0018 | 16.7% | 0.0220 | 0.0332 | 8.7 |
| **10** | 0.0015 – 0.0020 | 25.0% | 0.0267 | 0.0377 | 7.5 |
| **11** | 0.0015 – 0.0021 | 28.6% | 0.0249 | 0.0724 | 8.3 |
| **12** | 0.0011 – 0.0019 | 42.1% | 0.0238 | 0.0237 | 9.2 |
| **13** | 0.0030 – 0.0033 | 9.1% | 0.0392 | 0.0965 | 7.8 |
| **14** | 0.0010 – 0.0018 | 44.4% | 0.0192 | 0.0304 | 8.3 |
| Average | 0.0012 – 0.0019 | 42.4% | | | |

[a] All DFT calculations employed ORCA 5.0 using the PBE/def2-TZVP computational method.
[b] All atoms were refined anisotropically, with the exception of **3** and **13**, which implement disorder models. In structure **3**, all H atoms of the disordered molecule (the second molecule of the asymmetric unit) are refined isotropically in both components of the disorder model. In structure **13**, only the H atom involved in the minor component of the disorder model (H9) is refined isotropically.
[c] C-C bond precision taken from the CheckCIF Report. First value given is C-C bond precision in Å from structures refined using NoSpherA2, second value is from structures refined to IAM.

The successful HAR/NoSpherA2 treatment of all 14 structures, with a sufficiently high data-to-parameter ratio to enable good quality anisotropic displacement parameters of all ordered atoms, enabled accurate placement of H atom positions. Only the H atoms in the minor components of the two-part disorder model of **13**, and in the disordered and distorted molecule of **3**, were refined isotropically and were also excluded from statistical comparisons. The quality of these displacement models is evident from Figs. 1 – 4. Regarding the accuracy of the C–H bond distances, we have undertaken a statistical analysis with comparison to a 2010 survey of available neutron diffraction data in the CSD over various measurement temperature ranges.[112] The C-H bond distances of **1** – **14** as calculated using NoSpherA2 are in very good agreement with the neutron diffraction data (Table 6). Of the 150 C-H bonds in our structures, 134 are statistically similar at a 99% confidence level to the categorical average C-H bond length from neutron data (Tables S5-S19 in the SI).

**Table 6**. Comparison of C-H bond lengths from this work with values from neutron diffraction.

| C–H bond type | IAM standard values (AFIX @ 100 K)/ Å | % dev. (neutron) | **1** – **14**,[a] d /Å | *n* | % dev. (neutron) | Neutron Data $60 \le T \le 140$ K,[b] d /Å | *n* |
|---|---|---|---|---|---|---|---|
| $Z_3$-C$sp^3$-H | 1.00 | 9.0 | 1.077 (14) | 28 | 2.0 | 1.099 (7) | 66 |
| $Z_2$-C$sp^3$-$H_2$ | 0.99 | 8.9 | 1.090 (18) | 10 | 0.6 | 1.097 (6) | 136 |
| C$sp^2$ or C(ar)-H | 0.95 | 8.3 | 1.075 (16) | 112 | 0.9 | 1.085 (9) | 184 |

[a] This work. Errors are std. dev. of the sets of values. [b] Allen, F. H., Bruno, I. J.; *Acta Crystallogr B,* **2010**, *66* (Pt 3), 380-6

Figure 5 details the distribution of C-H bond lengths found in **1 – 14**, which are most commonly in the 1.04 – 1.10 Å range. The distribution is quite symmetrical for the $C_{Ar}$–H and C$sp^2$–H bonds, for which the mean value is also close to that reported from neutron data (Table 6), but more poorly defined for the aliphatic C–H bonds. The $Z_3$-C$sp^3$–H are in poorest agreement, while the number of determinations for $Z_2$-C$sp^3$–H is noticeably small. This, and our previous work,[58] suggest a possible trend of somewhat shorter C–H distances than from neutron data over similar temperature ranges. There is no inherent reason for the two techniques to deliver the same values, but as demonstrated from Table 6, this HAR approach is 5 to 15 times closer to the (neutron) reality than the fully constrained 'riding-atom' model that is ubiquitously employed in the IAM.

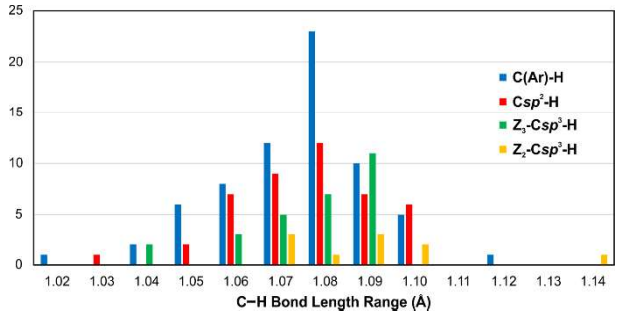


**Figure 5**. Histogram of C-H bond lengths for the different types of carbons in compounds **1 – 14**

**Analysis of C–H···N≡C non-classical H-bonding and dipolar C≡N···C≡N interactions in 2 – 14**

Dunitz's skepticism about the significance of any interactions weaker than classical H-bonding[113] has been resolutely countered by Lecomte et al,[114] by a consideration of the electron density distribution, and the Laplacian thereof, which affects *all* interatomic interactions, within and between molecules and ions. In other words, the strengths of intermolecular interactions are on a smooth gradient from the smallest to the largest interaction energies; consequently frequency matters. Many small interactions in composite can merge to overcome a single 'obviously' stronger interaction. Evidence for C–H···N≡C H-bonding has been obtained from vibrational spectroscopy.[115]

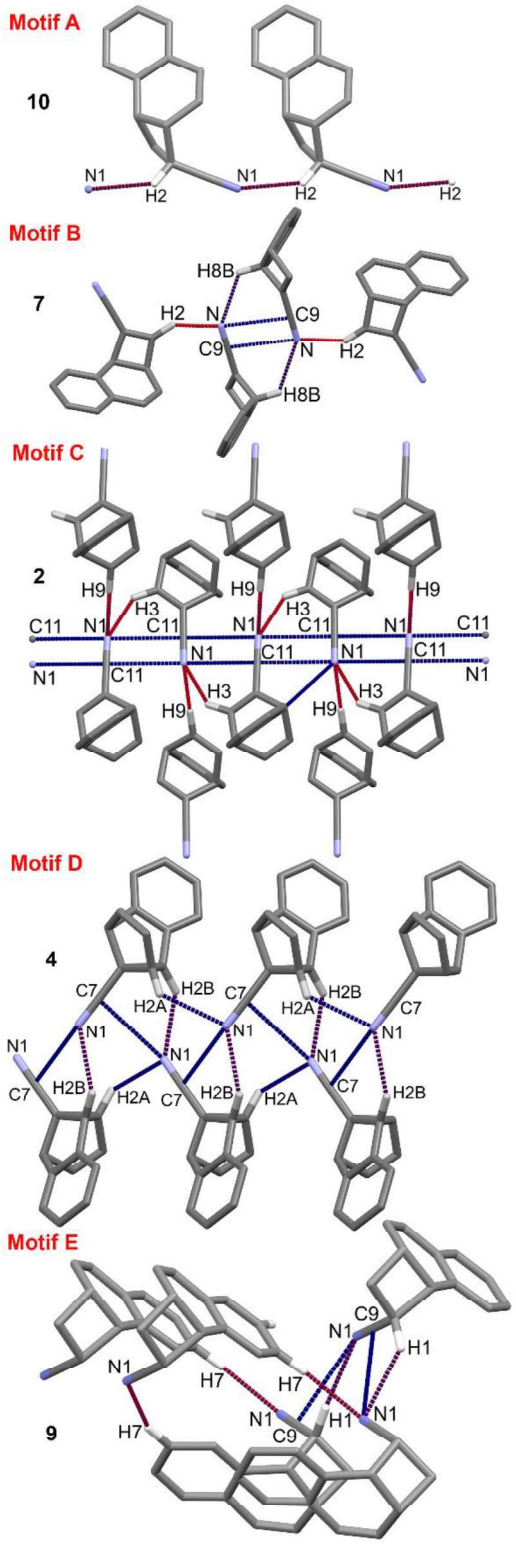


**Figure 6**. Five motifs encountered from combinations of -C≡N···H–C bonds and dipolar C≡N···C≡N interactions.

**Table 7**. Table of C–H···N≡C non-classical H-bonding and dipolar C≡N···C≡N interactions

| Comp. | Contact[a] | d(D-H)/Å | d(H-A)/Å | d(H-A)-$r_{vdW}$[b] | d(D-A)/Å | D-H···A/°[c] | Description |
|---|---|---|---|---|---|---|---|
| **2** | C3–H3···N1[1] | 1.08(3) | 2.37(3) | -0.38 | 3.296(3) | 142(2) | Terminal bifurcated |
| | C11···N1[1] | — | — | +0.08 | 3.326(3) | 97.1(1) | *Sheared antiparallel* |
| | N1···C11[1] | — | — | +0.12 | 3.369(3) | 94.9(1) | *Sheared antiparallel* |
| | C9–H9···N1[2] | 1.08(2) | 2.38(2) | -0.37 | 3.452(2) | 174(2) | Terminal bifurcated |
| **3** | C3-H3···N1[3] | 1.083(6) | 2.530(6) | -0.22 | 3.2332(7) | 121.7(4) | Terminal net forming |
| | C23-H23···N2[4] | 1.07(1) | 2.41(1) | -0.13 | 3.383(2) | 150.8(9) | Dimer forming |
| | N1···C2N[4] | — | — | 0.00 | 3.248(1) | 94.19 (4) | *Sheared antiparallel* |
| | C1N···N2[4] | — | — | +0.02 | 3.2663(8) | 93.27(6) | *Sheared antiparallel* |
| | N2···C2N[4] | — | — | +0.31 | 3.555(1) | 91.97 (6) | *Sheared antiparallel* |
| **4** | C2A-H2A···N1[2] | 1.070(4) | 2.715(5) | +0.04 | 3.4014(4) | 121.7(3) | Terminal bifurcated |
| | C2B-H2B···N1[5] | 1.063(4) | 2.575(4) | -0.08 | 3.4651(4) | 140.9(3) | Terminal bifurcated |
| | N1···C7[5] | — | — | +0.13 | 3.3874(4) | — | *Perpendicular nitrile* |
| **6** | C8-H8···N1[6] | 1.075(4) | 2.618(4) | -0.13 | 3.4846(4) | 137.3(3) | Chain forming |
| **7** | C2-H2···N[7] | 1.063(5) | 2.350(5) | -0.40 | 3.2195(6) | 138.1(4) | Links between dimers |
| | C8B-H8B···N[8] | 1.082(4) | 2.628(5) | -0.12 | 3.3771(6) | 125.3(3) | Dimer forming |
| | N···C9[8] | — | — | -0.01 | 3.2406(6) | 94.11(3) | *Sheared antiparallel* |
| **8** | C3-H3···N[9] | 1.077(3) | 2.762(3) | +0.12 | 3.4989(5) | 125.5(2) | Dimer forming |
| | N···C9[9] | — | — | +0.12 | 3.3740(5) | 85.17(2) | *Sheared antiparallel* |
| **9** | C7-H7···N1[10] | 1.083(12) | 2.470(13) | -0.18 | 3.4784(14) | 154(11) | Terminal net forming |
| | C1-H1···N1[2] | 1.091(11) | 2.578(11) | -0.07 | 3.4498(11) | 136.2(8) | Simple chain forming |
| | N1···C9[5] | — | — | +0.31 | 3.561(1) | 105.81(7) | *Sheared parallel* |
| **10** | C2-H2···N1[11] | 1.066(10) | 2.516(10) | -0.23 | 3.3827(12) | 137.7(8) | Simple chain forming |
| **11** | C6C-H6C···N11[15] | 1.09(1) | 2.51(1) | -0.24 | 3.562(1) | 163.2(7) | Terminal net forming |
| | C3-H3···N12[12] | 1.08(1) | 2.60(1) | -0.14 | 3.393(1) | 130.2(7) | Terminal net forming |
| | C16C-H16C···N1[13] | 1.07(1) | 2.61(1) | -0.14 | 3.673(2) | 169.7(7) | Terminal net forming |
| | C12A-H12A···N11[14] | 1.09(1) | 2.63(1) | -0.12 | 3.529(1) | 139.3(7) | Terminal net forming |
| | N2·· ·C18[10] | — | — | +0.06 | 3.312(1) | 96.17(7) | *Perpendicular nitrile* |
| | N11···C18[14] | — | — | +0.24 | 3.488(1) | 86.48(7) | *Perpendicular nitrile* |
| **12** | C9-H9···N4[15] | 1.083(9) | 2.426(9) | -0.34 | 3.2905(9) | 135.8(7) | Terminal bifurcated |
| | C13-H13···N1[17] | 1.09(1) | 2.46(1) | -0.29 | 3.468(1) | 152.8(8) | Terminal bifurcated |
| | C11-H11···N3[16] | 1.09(1) | 2.46(1) | -0.29 | 3.496(1) | 157.8(8) | Terminal bifurcated |
| | C20-H20···N3[20] | 1.09(1) | 2.55(1) | -0.20 | 3.347(1) | 121.7(7) | Terminal bifurcated |
| | C16-H16···N1[18] | 1.073(9) | 2.550(9) | -0.20 | 3.3067(9) | 126.8(8) | Terminal bifurcated |
| | C12-H12···N2[17] | 1.08(1) | 2.57(1) | -0.19 | 3.569(1) | 154.6(8) | Terminal bifurcated |
| | C15-H15···N1[18] | 1.098(9) | 2.635(9) | -0.12 | 3.3616(9) | 123.1(7) | Terminal bifurcated |
| | C15-H15···N4[19] | 1.098(9) | 2.68(1) | +0.07 | 3.468(1) | 128.1(7) | Terminal bifurcated |
| | N3···C1N-N1[4] | — | — | +0.16 | 3.413(1) | 104.15(6) | *Perpendicular nitrile* |
| **13** | C2A-H2A···N1[10] | 1.09(2) | 2.69(2) | -0.06 | 3.413(3) | 123(1) | Chain forming |
| | N1···C9-N1[10] | — | — | +0.09 | 3.336(3) | 84.8(1) | *Perpendicular nitrile* |
| **14** | C10-H10···N1[20] | 1.08(2) | 2.45(2) | -0.30 | 3.517(1) | 168(1) | Dimer forming |

[a] Symmetry codes: [1] 1-X,-1/2+Y,2-Z; [2] -1+X,+Y,+Z; [3] 3/2-X,-1/2+Y,1/2-Z; [4] 1-X,1-Y,1-Z; [5] -1/2+X,3/2-Y,1-Z; [6] -1+X,-1+Y,+Z; [7] -1/2+X,1/2-Y,-1/2+Z; [8] -X,-Y,1-Z; [9] -X,2-Y,1-Z; [10] -1/2+X,1/2-Y,1-Z; [11] +X,-1+Y,+Z; [12] 1/2+X,1/2-Y,1-Z; [13] 1/2-X,-Y,-1/2+Z; [14] 1/2-X,-1/2+Y,+Z; [15] +X,+Y,+Z; [16] +X,1/2-Y,-1/2+Z; [17] 1-X,-Y,1-Z; [18] 1+X,+Y,1+Z; [19] -X,-1/2+Y,1/2-Z; [20] 1+X,1/2-Y,1/2+Z; [20] 2-X,1-Y,1-Z.
[b] d(D-A)-$r_{vdW}$ in the case of dipolar C≡N···C≡N interactions. [c] N···C-N/° in the case of dipolar C≡N···C≡N interactions.

A fine-tuned consideration of C–H···N≡C short contacts, interpreted by a thorough computational analysis, has been undertaken by Luschtinetz et al.[116] on a set of nitrile-functionalized thiophene oligomers. The interaction energy of non-classical C–H···N≡C H-bonds was computed to be −21.7 kJ/mol and the interaction angle ∠C–H···N≡C was found to be close to 150° and the H···N distance to be 2.43 Å (at the MP2/cc-pvdz level of theory).[116] This places the interaction in the low-end of 'moderate H-bonds' by energy on the scale of Jeffrey, but in the (expected) 'weak H-bond' range according to distance (see Table S21). A retrospective analysis recognizes that weak H-bonds of this type cannot compete with stronger

structure-directing factors (including strong dispersion forces), but that in the absence of other mechanisms, we may expect C–H···N≡C H-bonding to contribute to structure direction.[117] A survey of the CSD was undertaken on all organic nitrile to C–H short contacts out to ($\sum r_{vdW}$ + 0.1Å) found several thousand hits, but no evidence of a maximum in the distance distribution indicative of a definitive supramolecular contact. The interaction angle ∠C–H···N≡C did show a broad distribution with a maximum at ~136 (20)°, also fitting the moderate interaction pattern of Jeffrey (Table S21). Wood *et al.* have analyzed the CSD for dipolar C≡N···C≡N interactions in structures of organic nitriles, in view of the high polarity of these functional groups.[78] Three distinct interaction geometries were identified, namely the sheared antiparallel (most common; with simultaneous contacts of each $N^{\delta-}$ to $C^{\delta+}$), perpendicular, and sheared parallel (each with contacts from a single $N^{\delta-}$ to $C^{\delta+}$ - see Fig. S1). A search for such contacts in our structures indicates that they are often found cooperatively with the H-bonding.

The most important non-classical C–H···N≡C H-bonds in the lattices of **2** – **14**, based on d(H···A)-$r_{vdW}$ and largest ∠H···N≡C, are listed in Table 7, with a description of their chief features. Five motifs have been determined from the combination of these interactions with dipolar C≡N···C≡N interactions, for which the optimal *d*(C···N) = 3.30 Å, being primarily electrostatic, is effectively the $\sum r_{vdW}$, as determined by Wood et al.[78] In all, nine of the thirteen nitrile structures show one of the three types of dipolar nitrile-nitrile contacts, which is a much higher fraction than the global average of 37% reported by these authors.[78] Since **8** has such a dipolar nitrile contact, the weak H-bond that correlates with it is included in Table 7, whereas **5** has been excluded for a total absence of contacts shorter than $\sum r_{vdW}$ – 0.1 Å.

**Motif A** (Figure 6) consists of a single chain-forming series of C–H···N≡C H-bonds, as illustrated in the lattice structure of **10**. There are no dipolar nitrile contacts. This motif is also found in the lattice of **6** (Figure S2 in the Supporting Information).

**Motif B**, illustrated best by the lattice structure of **7** (Figure 6), is a discrete dimer of sheared antiparallel (SAP) nitriles, supported further by a matching pair of C8BH8B···N≡C H-bonds. Extension of the motif occurs via the considerably stronger C2H2···N≡C H-bonds linking the dimers into chains. This motif is also present in the lattice structure of **8** (without the second, external link) and **3** (where there are quads from two sets of SAP nitriles) and, geometrically, also in **14** where the dimer is supported on the H-bonds because here the nitriles are too far apart to interact significantly (Table 7 and Figure S2).

**Motif C**, found in the lattice of **2** (Figure 6), is a further variant on **B**, wherein strong SAP nitrile contacts form an infinite ribbon with equal contact distances, supported again by bridging C3H3···N≡C H-bonds; contacts between ribbons are maintained by C9H9···N≡C H-bonds of comparable strength.

**Motif D** exemplifies perpendicular nitrile contacts, which in the lattice of **4** produces another continuous ribbon structure analogous to that of **2**, supported by double bridging H-bonds (Figure 6). Other exemplars of this motif can be found in the lattices of **11**, **12** and **13**, also with a simple continuous ribbon in **14**. As may be expected, the dinitriles **11** and **12** have, in addition to these perpendicular chain-forming nitrile interactions, many additional H-bonds leading to complex 3D networks (Table 7 and Figure S2).

**Motif E** contains the only sheared parallel nitrile interaction, found in the lattice of **9**, where it is also ribbon forming and supported by a bridging H-bond (Figure 6). A second terminal H-bond provides links to adjacent ribbons. While similar to the most common **motif C**, it differs by the angle of interaction between the nitrile moieties.

**Table 8**. Crystal data and structure refinement parameters for crystal structures of **1 – 14**

| **Parameter** | **1** | **2** | **3** | **4** | **5** | **6** | **7** |
|---|---|---|---|---|---|---|---|
| Chemical Formula | $C_{12}H_9Br$ | $C_{13}H_9N$ | $C_{13}H_{11}N$ | $C_{13}H_9N$ | $C_{13}H_9N$ | $C_{13}H_9N$ | C13H9N |
| Formula Weight (g/mol) | 233.109 | 179.223 | 181.239 | 179.223 | 179.223 | 179.223 | 179.223 |
| Temperature (K) | 173 | 173 | 100 | 173 | 173 | 173 | 173 |
| Crystal System | orthorhombic | monoclinic | monoclinic | orthorhombic | orthorhombic | triclinic | monoclinic |
| Space Group | $Pca2_1$ | $P2_1$ | $P2_1/n$ | $P2_12_12_1$ | $P2_12_12_1$ | $P\bar{1}$ | $P2_1/n$ |
| A (Å) | 18.8566(13) | 8.1796(5) | 10.9643(2) | 5.5108(1) | 7.0407(2) | 6.5819(2) | 8.4209(7) |
| b (Å) | 7.8568(6) | 6.4120(4) | 8.3710(2) | 9.1248(2) | 9.4027(2) | 7.5472(2) | 13.0840(11) |
| c (Å) | 6.3785(5) | 9.1633(6) | 21.4696(4) | 17.5736(4) | 14.1692(3) | 10.2062(3) | 9.3215(8) |
| A (°) | 90 | 90 | 90 | 90 | 90 | 106.310(2) | 90 |
| β (°) | 90 | 100.496(6) | 101.356(2) | 90 | 90 | 97.187(2) | 112.354(1) |
| γ (°) | 90 | 90 | 90 | 90 | 90 | 101.294(2) | 90 |
| Volume (Å$^3$) | 944.99(12) | 472.55(5) | 1931.95(7) | 883.69(3) | 938.02(4) | 468.35(3) | 949.85(14) |
| Z | 4 | 2 | 8 | 4 | 4 | 2 | 4 |
| Z' | 1 | 1 | 2 | 1 | 1 | 1 | 1 |
| $R_1$[a] [I ≥ 2σ(I)] | 0.0181 | 0.0270 | 0.0168 | 0.0092 | 0.0199 | 0.0120 | 0.0143 |
| $wR_2$ [all data] | 0.0323 | 0.0496 | 0.0337 | 0.0211 | 0.0426 | 0.0307 | 0.0311 |
| Twin[a]; major fraction | 0.921(6) | 0.618[b] | — | — | — | — | — |
| CCDC | 2112984 | 2112985 | 2112987 | 2112986 | 2112990 | 2112992 | 2112993 |
| **Parameter** | **8** | **9** | **10** | **11** | **12** | **13** | **14** |
| Chemical Formula | $C_{13}H_9N$ | $C_{13}H_{11}N$ | $C_{13}H_{11}N$ | $C_{14}H_8N_2$ | $C_{14}H_8N_2$ | $C_{17}H_{11}N$ | $C_{17}H_{11}N$ |
| Formula Weight (g/mol) | 179.223 | 181.239 | 181.239 | 204.233 | 204.233 | 229.283 | 229.283 |
| Temperature (K) | 173 | 100 | 173 | 173 | 100 | 173 | 100 |
| Crystal System | monoclinic | orthorhombic | monoclinic | orthorhombic | monoclinic | orthorhombic | monoclinic |
| Space Group | $P2_1/c$ | $P2_12_12_1$ | $P2_1/n$ | Pbca | $P2_1/c$ | $P2_12_12_1$ | $P2_1/c$ |
| A (Å) | 8.8036(7) | 5.7696(1) | 9.3073(6) | 11.7370(9) | 12.3616(4) | 5.5530(11) | 13.7748(6) |
| b (Å) | 10.3463(8) | 8.2484(1) | 5.6081(3) | 13.8928(10) | 13.2693(4) | 8.9395(18) | 8.1983(3) |
| c (Å) | 10.8587(8) | 20.6639(3) | 18.3728(11) | 24.4482(18) | 13.5889(4) | 22.594(5) | 11.4516(5) |
| A (°) | 90 | 90 | 90 | 90 | 90 | 90 | 90 |
| β (°) | 110.844(1) | 90 | 101.384(6) | 90 | 111.485(4) | 90 | 114.501(5) |
| γ (°) | 90 | 90 | 90 | 90 | 90 | 90 | 90 |
| Volume (Å$^3$) | 924.33(12) | 983.39(3) | 940.12(10) | 3986.5(5) | 2074.10(12) | 1121.6(4) | 1176.78(10) |
| Z | 4 | 4 | 4 | 16 | 8 | 4 | 4 |
| Z' | 1 | 1 | 1 | 2 | 2 | 1 | 1 |
| $R_1$[a] [I ≥ 2σ(I)] | 0.0121 | 0.0220 | 0.0267 | 0.0249 | 0.0238 | 0.0392 | 0.0192 |
| $wR_2$ [all data] | 0.0241 | 0.0566 | 0.0440 | 0.0350 | 0.0531 | 0.0643 | 0.0369 |
| Twin; major fraction | — | 0.602 | — | — | — | — | — |
| CCDC | 2112988 | 2112989 | 2112991 | 2112994 | 2112996 | 2112995 | 2112997 |

[a] Racemic twin refinement except **2**. [b] Twin integration in CrysAlisPro, 2-fold rotation around [0.98 -0.00 -0.20] in reciprocal space.

## CONCLUSIONS

In this paper, we have shown that HAR can be applied to a set of average to good quality, 'standard resolution' crystallographic datasets. In all cases, it was possible to refine atom positions and to model ADPs for H-atoms with limited restraints, and in the best cases, fully unrestrained refinements were possible. The most important outcomes of our study are the trends derived from Table 5, indicating improvement in overall structure precision in *all fourteen* structure models compared to employing an equivalent IAM refinement. Moreover, this data shows that the greatest improvement in accuracy comes with the highest quality datasets, but also that no discontinuities occur. In other words, there does not seem to be a downside to routinely employing the HAR/NoSpherA2 approach, with the expectation that the best standard- or higher-resolution datasets will afford the greatest improvement in accuracy versus equivalent IAM refinement. Many of the structures of the valence isomers reported in this work significantly increase the numbers of exemplars in rare organic structure classes.

## EXPERIMENTAL

**General Methods**. The sources of all the compounds used in this study have been outlined under Chemical Background. Crystals suitable for single-crystal X-ray diffraction were obtained by slow cooling to ambient temperature from the following solvents: **1** from cyclohexane; **2, 4, 5, 6, 13** and **14** from ethanol; **3, 7**, **8**, **9** and **10** from hexane; **11** methanol; and **12** from acetone/hexane.

**Crystallography**. Crystals were selected under a polarizing microscope and checked for optical extinction. Colorless crystals were mounted in Paratone™ oil either on the ends of thin capillaries or on a 100 µm MiTeGen loop and cooled to 173 (2) or 100 (1) K using the diffractometer cooling devices (Bruker Kryoflex or Oxford Cryostream 800, respectively). Data were collected either on Bruker ApexII CCD (Mo Kα) or Rigaku-Oxford Diffraction SuperNova HPC (Cu Kα) diffractometers. Data collection and reduction was controlled, respectively, with *SAINT-Plus* or CrysAlisPro 1.171.38.43 (Rigaku Oxford Diffraction, 2021). The data were processed and corrected for Lorentz and polarization effects by standard methods and corrected for absorption by semi-empirical methods from equivalents. Structures were solved with shelXS[118] or shelXT[119] and refined using Levenberg–Marquardt minimization with olex2.refine[55] within the Olex2 suite.[105] The refinements employed NoSpherA2, (NOn-SPHERical Atom-form-factors in Olex2)[56] an implementation of HAR that makes use of tailor-made aspherical atomic scattering factors calculated on-the-fly from a Hirshfeld-partitioned electron density (ED). The ED is calculated from a Gaussian basis set single determinant SCF wavefunction in DFT at the PBE/def2-TZVP level of theory using ORCA 5.0.[120] The CIF files of the finalized structures of **1** – **14** and of the structures of the comparators collected from the CSD were run through the PLATON crystallographic software suite[109-110] to extract the Cremer puckering parameters and least-squares planes values. Crystal data and structure refinement parameters are summarized in Table 8, and full archival data is available in CIF format.

Importantly, CIFs prepared from within Olex2 contain a detailed reporting of every facet of modelling. Only the briefest summary, expanding on the standard parameters listed in Table 8, can be provided here. The structure of **1** was refined as an inversion twin in the non-centrosymmetric space group $Pca2_1$. Mild ISOR restraints were applied to the ADPs of H3, 6, 7, and 10. The crystal employed for the structure of **2** was twinned and integrated as a two-component twin in space group $P2_1$ (0.62:0.38 ratio), which resulted in a slightly low completeness in the outermost shell. Mild ISOR restraints were applied to ADPs for seven H-atoms, and stronger ISOR on atoms H1,4. Eight strongly outlying data were omitted. The structure of **3** in centrosymmetric space group $P2_1/n$ has $Z' = 2$, and the second molecule is

severely disordered. A satisfactory two-part refinement model was applied with standard geometrical restraints. The disordered model employed isotropic H-atom refinements with restraints to the average C–H distances encountered in this study. The ordered molecule, used for all statistical comparisons, was refined without any restraints. The structure of **4** was determined from an excellent dataset with 98% completeness to $\sin\theta/\lambda = 0.67$ Å$^{-1}$, and an unrestrained refinement with H-atom positions and ADPs was performed. The same is true for the structure of **5**, and similarly for **6** but $\sin\theta/\lambda$ reached 0.69 Å$^{-1}$. The structures of **7** and **8** also refined well without restraints, but the data was limited to $\sin\theta/\lambda = 0.60$ Å$^{-1}$. The structure of **9** was determined with Cu $K_\alpha$ radiation and refined without restraints to $\sin\theta/\lambda = 0.63$ Å$^{-1}$, while that of **10** and **11** was limited to $\sin\theta/\lambda = 0.60$ Å$^{-1}$ using Mo $K_\alpha$ radiation. The structure of **12** employed Cu $K_\alpha$ radiation with 94% completeness to 0.63 Å$^{-1}$ and required strong ISOR restraints on the ADPs of H10,14, the only restraints employed. The dataset used for the structure of **13** suffered from a poor $R_{int}$ of 9.7%, and was limited to $\sin\theta/\lambda = 0.60$ Å$^{-1}$ using Mo $K_\alpha$ radiation. The crystal employed for data collection was highly anisotropic, but all attempts to cut crystals to a reasonable length/width ratio resulted in splintering into much thinner needles. It is thus possible that the selected data crystal was a closely aligned 'fibre bundle', possibly contributing to the high $R_{int}$. Mild ISOR was applied to all the H atoms ADPs except for H2A, for which a strong ISOR was applied. Finally, the data for the structure of **14** employed Cu $K_\alpha$ radiation with 97% completeness to 0.63 Å$^{-1}$, to which RIGU restraints were applied to all eleven H-atom ADPs in the main component, whilst the disordered H-atom was refined isotropically. The CN/H disorder was refined to an 80:20 ratio of major and minor components. The use of RIGU restraints in HAR has been carefully validated, and shown not to have a significant effect on the accuracy of H-atom positional refinement.[121] By way of a small warning, however, in the original version of this paper, some structures were accidentally treated with RIGU on the well-behaved C atoms as well as on the attached H atoms. An anonymous referee pointed out that removing such coupled-atom RIGU restraints significantly relaxed the geometries on further refinement, and our re-refinements confirmed this phenomenon. A full investigation of the origin of this effect is beyond the scope of this paper, but in future work we envisage comparing parallel treatment of H-atom ADPs with and without RIGU restraints in HAR/NoSpherA2 refinements.

## ASSOCIATED CONTENT

**Supporting Information.** The Supporting Information is available free of Charge at:

Tables of puckering parameters; Tables of statistical comparison of C-H bond lengths to neutron diffraction data; Analysis of 'short' C-H bond lengths (1.02 – 1.06 Å) in **1** – **14**; Ranking of hydrogen bond strengths following Jeffrey; Bond length and angle data for Type II structures. Figure of three commonly observed C≡N···C≡N interaction motifs from Wood et al.; Figure of combined nitrile dipolar contacts and non-classical -C≡N···H−C bonds; Figure of correlation of model quality and % improvement in C–C bond precision

**Accession Codes**. CCDC 2112984–2112997 contain the supplementary crystallographic data for this paper. These data can be obtained free of charge via www.ccdc.cam.ac.uk/data_request/cif, or by emailing data_request@ccdc.cam.ac.uk, or by contacting The Cambridge Crystallographic Data Centre, 12 Union Road, Cambridge CB2 1EZ, UK; fax: +44 1223336033.

**ACKNOWLEDGEMENTS**

This work was underwritten by ongoing Discovery Grants from the Natural Sciences and Engineering Research Council (NSERC) and by a generous grant from the University of Lethbridge Research Fund (ULRF). The diffractometer at the University of Lethbridge X-ray Diffraction Facility was purchased by the University and the Faculty of Arts & Science.

**REFERENCES**

1. Maier, J.; Deutsch, M.; Merz, J.; Ye, Q.; Diamond, O.; Schilling, M. T.; Friedrich, A.; Engels, B.; Marder, T. B., Highly Conjugated pi-Systems Arising from Cannibalistic Hexadehydro-Diels-Alder Couplings: Cleavage of C-C Single and Triple Bonds. *Chem. - Eur. J.* **2020,** *26* (68), 15989-16000.
2. Kremlev, M. M.; Mushta, O. I.; Yagupolskii, Y. L.; Rusanova, J. A.; Peng, S.; Petrov, V., Synthesis of 9,10-bis(trifluoromethyl)benzobarrelenes through reaction of hexafluorobut-2-yne and substituted naphthalenes. *J. Fluorine Chem.* **2020,** *232*, 109450.
3. Schlesinger, M.; Hofmann, M.; Ruffer, T.; Schaarschmidt, D.; Lang, H.; Theilacker, S.; Schurmann, M.; Jurkschat, K.; Mehring, M., Synthesis of Dibromobenzobarrelene Derivatives and Catalytic Activity of Their Rhodium Complexes. *Eur. J. Inorg. Chem.* **2013**, 2930 - 2939.
4. Nikitin, K.; Müller-Bunz, H.; McGlinchey, M. J., Diels–Alder Reactions of 9-Ferrocenyl- and 9,10-Diferrocenylanthracene: Steric Control of 9,10- versus 1,4-Cycloaddition. *Organometallics* **2013,** *32* (20), 6118-6129.
5. Kaya, A. A.; Sengul, M. E.; Menzek, A.; Kayaardi, I.; Karakus, M.; Sahin, E., Aromatisation in adducts of (alpha)-terpinene: Influence of hindered internal rotations. *J. Chem. Res.* **2011**, 540-544.
6. Goh, Y. W.; Danczak, S. M.; Lim, T. K.; White, J. M., Manifestations of the Alder-Rickert Reaction in the Structures of Bicyclo[2.2.2]octadiene and Bicyclo[2.2.2]octene Derivatives. *J. Org. Chem.* **2007,** *72*, 2929-2935.
7. Zimmerman, H. E.; Paufler, R. M., Bicyclo[2,2,2]-2,5,7-octatriene (Barrelene), a Unique Cyclic Six Electron Pi System. *J. Am. Chem. Soc.* **1960,** *82* (6), 1514-1515.
8. Groom, C. R.; Bruno, I. J.; Lightfoot, M. P.; Ward, S. C., The Cambridge Structural Database. *Acta Crystallogr., Sect. B: Struct. Sci., Cryst. Eng. Mater.* **2016,** *72* (2), 171-179.
9. Boeré, R. T.; Bender, C. O., A tetrabromo-1,4-ethanonaphthalene and related dibromo-1,4-ethenonaphthalene. *Acta Crystallogr., Sect. C: Struct. Chem.* **2013,** *69* (Pt 3), 247-250.
10. Bender, C. O.; O'Shea, S. F., Mechanistic and Theoretical Studies of the Photochemistry of 5,6-dihydro-2-cyanobenzobarrelene. *Can. J. Chem.* **1979,** *57*, 2804-2811.
11. Ryan, D. E., Stereoselective Synthesis of Concave Spacers for Long-Range Electron Transfer Models. *Tetrahedron Lett.* **1996,** *37* (34), 6089-6092.
12. Aotake, T.; Suzuki, M.; Aratani, N.; Yuasa, J.; Kuzuhara, D.; Hayashi, H.; Nakano, H.; Kawai, T.; Wu, J.; Yamada, H., 9,9'-Anthryl-anthroxyl radicals: strategic stabilization of highly reactive phenoxyl radicals. *Chem. Commun.* **2015,** *51* (31), 6734-6737.
13. Tanaka, K.; Aratani, N.; Kuzuhara, D.; Sakamoto, S.; Okujima, T.; Ono, N.; Uno, H.; Yamada, H., A soluble bispentacenequinone precursor for creation of directly 6,6′-linked bispentacenes and a tetracyanobipentacenequinodimethane. *RSC Adv.* **2013,** *3* (35), 15310-15315.
14. Mithani, S. W., Gamini; Taylor, Nicholas J.; Dmitrienko, Gary I., The Kinamycins are Diazofluorenes and not Cyanocarbazoles. *J. Am. Chem. Soc.* **1994,** *116*, 2209-2210.
15. Pogula, V. D.; Wang, T.; Hoye, T. R., Intramolecular [4 + 2] trapping of a hexadehydro-Diels-Alder (HDDA) benzyne by tethered arenes. *Org. Lett.* **2015,** *17* (4), 856-859.

16. Moazeni, A.; Bender, C. O.; Boeré, R. T., Dimethyl 7-methoxytetracyclo-[6.4.0.0(2,4).0(3,7)]dodeca-1(12),5,8,10-tetraene-3,4-dicarboxylate. *Acta Crystallogr., Sect. E: Crystallogr. Commun.* **2012,** *68* (10), o2837.
17. Jones, R.; Scheffer, J. R.; Trotter, J.; Yap, M., Crystal Structure and Photochemistry of Dimethyl 1,4-Dihydro-l,4,5,8-tetramethyl-1,4-ethenonaphthalene-2,3-dicarboxylate. *Acta Crystallogr., Sect. B: Struct. Sci., Cryst. Eng. Mater.* **1994,** *B50*, 597-600.
18. Pokkuluri, P. R.; Scheffer, J. R.; Trotter, J.; Yap, M., An Ethenonaphthalene and One of its Photolysis Products. *Acta Crystallogr., Sect. C: Struct. Chem.* **1994,** *C50*, 578-581.
19. Pokkuluri, P. R.; Scheffer, J. R.; Trotter, J., The Photolysis Product of Dimethyl-9,10-Diphenyl-1,4-dihydro-1,4-ethenoanthracene-11,12-dicarboxylate. *Acta Crystallogr., Sect. C: Struct. Chem.* **1994,** *C50*, 581-583.
20. Sajimon, M. C.; Ramaiah, D.; Kumar, S. A.; Rath, N. P.; George, M. V., Substituent Effects on Regioselectivity in the Photorearrangement of a Few Naphthobarrelenes. *Tetrahedron* **2000,** *56*, 5421-5428.
21. Şengül, M. E.; Gültekin, D. D.; Eşsiz, S.; Şahin, E.; Daştan, A., The first and efficient synthesis of some of the polyhalogenated benzobarrelenes: unusual formation of a benzosemibullvalene derivative. *Tetrahedron* **2009,** *65* (25), 4859-4865.
22. Berger, H.; Hopf, H.; Dix, I.; Jones, Peter G., A New Route for the Thermal Isomerization of a Highly Substituted Hexadienyne Derivative. *Eur. J. Org. Chem.* **2004,** *2004* (16), 3401-3403.
23. Edelmann, F. T.; Freckmann, D. M. M.; Schumann, H., Synthesis and Structural Chemistry of Non-Cyclopentadienyl Organolanthanide Complexes. *Chem. Rev.* **2002,** *102*, 1851-1896.
24. Roesky, P. W., Substituted Cyclooctatetraenes as Ligands in f-Metal Chemistry. *Eur. J. Inorg. Chem.* **2001**, 1653-1660.
25. Medel, M. A.; Tapia, R.; Blanco, V.; Miguel, D.; Morcillo, S. P.; Campana, A. G., Octagon-Embedded Carbohelicene as a Chiral Motif for Circularly Polarized Luminescence Emission of Saddle-Helix Nanographenes. *Angew. Chem., Int. Ed.* **2021,** *60* (11), 6094-6100.
26. Urieta-Mora, J.; Krug, M.; Alex, W.; Perles, J.; Fernandez, I.; Molina-Ontoria, A.; Guldi, D. M.; Martin, N., Homo and Hetero Molecular 3D Nanographenes Employing a Cyclooctatetraene Scaffold. *J. Am. Chem. Soc.* **2020,** *142* (9), 4162-4172.
27. Pun, S. H.; Wang, Y.; Chu, M.; Chan, C. K.; Li, Y.; Liu, Z.; Miao, Q., Synthesis, Structures, and Properties of Heptabenzo[7]circulene and Octabenzo[8]circulene. *J. Am. Chem. Soc.* **2019,** *141* (24), 9680-9686.
28. Pun, S. H.; Miao, Q., Toward Negatively Curved Carbons. *Acc. Chem. Res.* **2018,** *51* (7), 1630-1642.
29. Marquez, I. R.; Castro-Fernandez, S.; Millan, A.; Campana, A. G., Synthesis of distorted nanographenes containing seven- and eight-membered carbocycles. *Chem. Commun.* **2018,** *54* (50), 6705-6718.
30. Cheung, K. Y.; Chan, C. K.; Liu, Z.; Miao, Q., A Twisted Nanographene Consisting of 96 Carbon Atoms. *Angew. Chem., Int. Ed.* **2017,** *56* (31), 9003-9007.
31. Sakamoto, Y.; Suzuki, T., Tetrabenzo[8]circulene: aromatic saddles from negatively curved graphene. *J. Am. Chem. Soc.* **2013,** *135* (38), 14074-14077.
32. Bello-Garcia, J.; Padin, D.; Varela, J. A.; Saa, C., Nonplanar Tub-Shaped Benzocyclooctatetraenes via Halogen-Radical Ring Opening of Dihydrobiphenylenes. *Org. Lett.* **2021,** *23* (14), 5539-5544.
33. Korovina, N. V.; Chang, M. L.; Nguyen, T. T.; Fernandez, R.; Walker, H. J.; Olmstead, M. M.; Gherman, B. F.; Spence, J. D., Syntheses and Reactivity of Naphthalenyl-Substituted Arenediynes. *Org. Lett.* **2011,** *13* (14), 3660-3663.
34. Liu, Q., N-Methyl-1,2-diphenylcyclobuteno[3,4-a]naphthalene-2,3-dicarboximide. *Acta Crystallogr., Sect. E: Crystallogr. Commun.* **2007,** *63* (6), o2901-o2901.

35. Liu, Q.-J.; Shen, Y.-M.; An, H.-Y.; Grampp, G.; Landgraf, S.; Xu, J.-H., Photoinduced cycloadditions of N-methyl-1,8-naphthalenedicarboximides with alkynes. *Tetrahedron* **2006,** *62* (6), 1131-1138.
36. Shen, Y.-M.; Lu, Z.-F.; Liu, Y.; Xu, J.-H., 1,4-Dimethyl-2-phenyl-3H,10aH-4-azacyclobuta[c]phenylene-3,5-dione. *Acta Crystallogr., Sect. E: Crystallogr. Commun.* **2005,** *61* (11), o3950-o3952.
37. Liu, Q.-J.; Xu, J.-H., 9-Bromo-4-methyl-2-phenylbenzo[de]cyclobut[i]isoquinoline-3,5(2H)-dione. *Acta Crystallogr., Sect. E: Crystallogr. Commun.* **2004,** *60* (3), o466-o467.
38. Liu, Q.; Qu, R.; Xu, J., 2-(4-Methoxyphenyl)-4-methylbenzo[de]cyclobut[i]isoquinoline-3,5(2H)-dione. *Acta Crystallogr., Sect. E: Crystallogr. Commun.* **2003,** *59* (9), o1246-o1248.
39. Liu, Q. S., Daqing; Xu, Jianhua, Crystal structure of 4-methyl-2-phenylbenzo[de]cyclobut[i]isoquinoline-3,5(2H)-dione. *J. Chem. Crystallogr.* **2003,** *33* (4), 263-267.
40. Maeda, H.; Takenaka, H.; Mizuno, K., Intermolecular hydrogen bonding controlled stereoselective photocycloaddition of vinyl ethers to 1-cyanonaphthalenes. *Photochem. Photobiol. Sci.* **2016,** *15* (11), 1385-1392.
41. Sakamoto, M.; Yagishita, F.; Saito, A.; Kobaru, S.; Unosawa, A.; Mino, T.; Fujita, T., Asymmetric photocycloaddition of naphthamide with a diene using the provisional molecular chirality in a chiral crystal. *Photochem. Photobiol. Sci.* **2011,** *10* (9), 1387-1389.
42. Mangion, D.; Frizzle, M.; Arnold, D. R.; Cameron, S., The Photochemistry of Acrylonitrile with Methoxylated Naphthalenes: Introducing the Photochemical Electrophile-Olefin Combination, Aromatic Substitution (Photo-EOCAS) Reaction. *Synthesis* **2001,** *8*, 1215-1222.
43. Yokoyama, A.; Mizuno, K., Stereoselective Photocycloaddition of Alkenes to Naphthalene Rings Assisted by Hydrogen Bonding. *Org. Lett.* **2000,** *2* (22), 3457-3459.
44. Dopp, D.; Erian, A. W.; Henkel, G., Light-Induced [2+2] Cycloaddition of 2-Morpholinoacrylonitrile to 1-Naphthalenecarbonitrile. *Chem. Ber.* **1993,** *126*, 239-242.
45. Matsuura, H.; Kai, Y.; Yasuoka, N.; Kasai, N., The Molecular Structure of 1-Phenoxy-1,2,2a,8b-tetrahydrocyclobuta(a)naphthalene-8b-carbonitrile. *Bull. Chem. Soc. Jpn.* **1980,** *53*, 359-361.
46. Bender, C. O.; Dolman, D.; Murphy, G. K., The photochemistry of 8-cyano-2,3-benzobicyclo[4.2.0]octa-2,4,7-triene. *Can. J. Chem.* **1988,** *66*, 1656-1662.
47. Bender, C. O.; Bengtson, D. L.; Dolman, D.; O'Shea, S. F., The photochemistry of 6- and 7-cyano-2,3-benzobicyclo[4.2.0]octa-2,4,7-triene. *Can. J. Chem.* **1986,** *64*, 237-245.
48. Bender, C. O.; Brooks, D. W.; Cheng, W.; Dolman, D.; O'Shea, S. F.; Shugarman, S. S., Polar substituents in barrelene photochemistry: mechanistic aspects of the photochemistry of 2-cyanobenzobarrelene. *Can. J. Chem.* **1978,** *56*, 3027-3037.
49. Bender, C. O.; Shugarman, S. S., Polar substituents in pericyclic reactions: photochemistry of 2-cyanobenzobarrelene. *J. Chem. Soc., Chem. Commun.* **1974,** (22), 934-935.
50. Bender, C. O.; Burgess, H. D., The Photochemistry of 2Cyano-1,4-dihydro-1,4-ethenoanthracene. *Can. J. Chem.* **1973,** *51*, 3486-3493.
51. McCullough, J. J.; Calvo, C.; Huang, C. W., The Photo-addition of Naphthalene and Acrylonitrile. *Chem. Commun.* **1968,** *19*, 1176-1177.
52. Woińska, M.; Grabowsky, S.; Dominiak, P. M.; Woźniak, K.; Jayatilaka, D., Hydrogen atoms can be located accurately and precisely by x-ray crystallography. *Science Advances* **2016,** *2* (5), e1600192.
53. Capelli, S. C.; Burgi, H. B.; Dittrich, B.; Grabowsky, S.; Jayatilaka, D., Hirshfeld atom refinement. *IUCrJ* **2014,** *1* (Pt 5), 361-379.
54. Farrugia, L. J., Accurate H-atom parameters from X-ray diffraction data. *IUCrJ* **2014,** *1* (Pt 5), 265-266.
55. Bourhis, L. J.; Dolomanov, O. V.; Gildea, R. J.; Howard, J. A.; Puschmann, H., The anatomy of a comprehensive constrained, restrained refinement program for the modern computing environment - Olex2 dissected. *Acta Crystallogr A Found Adv* **2015,** *71* (Pt 1), 59-75.

56. Kleemiss, F.; Dolomanov, O. V.; Bodensteiner, M.; Peyerimhoff, N.; Midgley, L.; Bourhis, L. J.; Genoni, A.; Malaspina, L. A.; Jayatilaka, D.; Spencer, J. L.; White, F.; Grundkotter-Stock, B.; Steinhauer, S.; Lentz, D.; Puschmann, H.; Grabowsky, S., Accurate crystal structures and chemical properties from NoSpherA2. *Chem. Sci.* **2020,** *12* (5), 1675-1692.
57. Bacon, G. E., *Neutron Diffraction (Third Edition)*. Oxford Eng. : Clarendon Press: 1975.
58. Marszaukowski, F.; Boeré, R. T.; Wohnrath, K., Frustrated and Realized Hydrogen Bonding in 4-Hydroxy-3,5-ditertbutylphenylphosphine Derivatives. *Cryst. Growth Des.* **2022,** *22* (4), 2512-2533.
59. Ibrahim, M. A.; Boeré, R. T., The copper sulfate hydration cycle. Crystal structures of CuSO4 (Chalcocyanite), CuSO4·H2O (Poitevinite), CuSO4·3H2O (Bonattite) and CuSO4·5H2O (Chalcanthite) at low temperature using non-spherical atomic scattering factors. *New J. Chem.* **2022,** *46* (12), 5479-5488.
60. Genoni, A.; Bucinsky, L.; Claiser, N.; Contreras-Garcia, J.; Dittrich, B.; Dominiak, P. M.; Espinosa, E.; Gatti, C.; Giannozzi, P.; Gillet, J. M.; Jayatilaka, D.; Macchi, P.; Madsen, A. O.; Massa, L.; Matta, C. F.; Merz, K. M., Jr.; Nakashima, P. N. H.; Ott, H.; Ryde, U.; Schwarz, K.; Sierka, M.; Grabowsky, S., Quantum Crystallography: Current Developments and Future Perspectives. *Chemistry* **2018,** *24* (43), 10881-10905.
61. Grabowsky, S.; Genoni, A.; Burgi, H. B., Quantum crystallography. *Chem. Sci.* **2017,** *8* (6), 4159-4176.
62. Langan, P.; Fisher, Z.; Kovalevsky, A.; Mustyakimov, M.; Sutcliffe Valone, A.; Unkefer, C.; Waltman, M. J.; Coates, L.; Adams, P. D.; Afonine, P. V.; Bennett, B.; Dealwis, C.; Schoenborn, B. P., Protein structures by spallation neutron crystallography. *J Synchrotron Radiat* **2008,** *15* (Pt 3), 215-218.
63. Maley, S. M.; Steagall, R.; Lief, G. R.; Buck, R. M.; Yang, Q.; Sydora, O. L.; Bischof, S. M.; Ess, D. H., Computational Evaluation and Design of Polyethylene Zirconocene Catalysts with Noncovalent Dispersion Interactions. *Organometallics* **2022,** *41* (5), 581-593.
64. Rösel, S.; Schreiner, P. R., Computational Chemistry as a Conceptual Game Changer: Understanding the Role of London Dispersion in Hexaphenylethane Derivatives (Gomberg Systems). *Isr. J. Chem.* **2022,** *62* (1-2), e202200002.
65. Riu, M. Y.; Bistoni, G.; Cummins, C. C., Understanding the Nature and Properties of Hydrogen-Hydrogen Bonds: The Stability of a Bulky Phosphatetrahedrane as a Case Study. *J. Phys. Chem. A* **2021,** *125* (28), 6151-6157.
66. Rosel, S.; Becker, J.; Allen, W. D.; Schreiner, P. R., Probing the Delicate Balance between Pauli Repulsion and London Dispersion with Triphenylmethyl Derivatives. *J. Am. Chem. Soc.* **2018,** *140* (43), 14421-14432.
67. Hill, N. D. D.; Boeré, R. T., Two tris-(3,5-disubstituted phen-yl)phosphines and their isostructural P(V) oxides. *Acta Crystallogr., Sect. E: Crystallogr. Commun.* **2018,** *74* (Pt 7), 889-894.
68. Dimbarre Lao Guimarães, I.; Garcia, J. R.; Wohnrath, K.; Boeré, R. T., Chemical and Electrochemical Oxidation of Tris(3,5-di-tert-butylphenyl)phosphine – High Z′ Crystal Structures and Conformational Effects Associated with Bulky meta Substituents. *Eur. J. Inorg. Chem.* **2018,** *2018* (32), 3606-3614.
69. de Almeida, L. R.; Carvalho, P. S.; Napolitano, H. B.; Oliveira, S. S.; Camargo, A. J.; Figueredo, A. S.; de Aquino, G. L. B.; Carvalho-Silva, V. H., Contribution of Directional Dihydrogen Interactions in the Supramolecular Assembly of Single Crystals: Quantum Chemical and Structural Investigation of C17H17N3O2 Azine. *Cryst. Growth Des.* **2017,** *17* (10), 5145-5153.
70. Ikawa, T.; Yamamoto, Y.; Heguri, A.; Fukumoto, Y.; Murakami, T.; Takagi, A.; Masuda, Y.; Yahata, K.; Aoyama, H.; Shigeta, Y.; Tokiwa, H.; Akai, S., Could London Dispersion Force Control Regioselective (2 + 2) Cyclodimerizations of Benzynes? YES: Application to the Synthesis of Helical Biphenylenes. *J. Am. Chem. Soc.* **2021,** *143* (29), 10853-10859.
71. Altun, A.; Neese, F.; Bistoni, G., HFLD: A Nonempirical London Dispersion-Corrected Hartree-Fock Method for the Quantification and Analysis of Noncovalent Interaction Energies of Large Molecular Systems dagger. *J. Chem. Theory Comput.* **2019,** *15* (11), 5894-5907.

72. Solel, E.; Ruth, M.; Schreiner, P. R., London Dispersion Helps Refine Steric A-Values: Dispersion Energy Donor Scales. *J. Am. Chem. Soc.* **2021,** *143* (49), 20837-20848.
73. Rosel, S.; Quanz, H.; Logemann, C.; Becker, J.; Mossou, E.; Canadillas-Delgado, L.; Caldeweyher, E.; Grimme, S.; Schreiner, P. R., London Dispersion Enables the Shortest Intermolecular Hydrocarbon H...H Contact. *J. Am. Chem. Soc.* **2017,** *139* (22), 7428-7431.
74. Corpinot, M. K.; Bučar, D.-K., A Practical Guide to the Design of Molecular Crystals. *Cryst. Growth Des.* **2018,** *19* (2), 1426-1453.
75. Desiraju, G. R., Crystal engineering: from molecule to crystal. *J. Am. Chem. Soc.* **2013,** *135* (27), 9952-67.
76. Gavezzotti, A.; Presti, L. L., Building Blocks of Crystal Engineering: A Large-Database Study of the Intermolecular Approach between C–H Donor Groups and O, N, Cl, or F Acceptors in Organic Crystals. *Cryst. Growth Des.* **2016,** *16* (5), 2952-2962.
77. Steiner, T., The Hydrogen Bond in the Solid State. *Angew. Chem., Int. Ed.* **2002,** *41*, 48-76.
78. Wood, P. A.; Borwick, S. J.; Watkin, D. J.; Motherwell, W. D.; Allen, F. H., Dipolar C[triple-bond]N...C[triple-bond]N interactions in organic crystal structures: database analysis and calculation of interaction energies. *Acta Crystallogr., Sect. B: Struct. Sci., Cryst. Eng. Mater.* **2008,** *64* (3), 393-6.
79. Bowman, R. M.; Chamberlain, T. R.; Huang, C. W.; McCullough, J. J., Medium Effects and Quantum Yields in the Photoaddition of Naphthalene and Acrylonitrile. Chemical Evidence on an Exciplex Structure. *J. Am. Chem. Soc.* **1974,** *96* (3), 692-700.
80. Unaldi, N. S.; Balci, M., Substituent effect on regioselectivity in the di--methane rearrangement: synthesis of disubstituted benzobarrelene derivatives and their photochemistry. *Tetrahedron Lett.* **2001,** *42*, 8365-8367.
81. Stout, G. H.; Jensen, L. H., *X-ray Structure Determination: A Practical Guide*. 2nd ed. John Wiley & Sons: N.Y., 1989.
82. Uno, H.; Furukawa, M.; Fujimoto, A.; Uoyama, H.; Watanabe, H.; Okujima, T.; Yamada, H.; Mori, S.; Kuramoto, M.; Iwamura, T.; Hatae, N.; Tani, F.; Komatsu, N., Porphyrin molecular tweezers for fullerenes. *J. Porphyrins Phthalocyanines* **2012,** *15*, 951-963.
83. Hart, H.; Du, C.-J. F.; Mohebalian, J., Aryne Cycloaddition to the Aromatic Ring of Mesitylmagnesium Bromide. An Anion-Assisted Diels-Alder Reaction? *Organometallics* **1988,** *32*, 6118-6129.
84. Trotter, J., Structure of Dimethyl 7,8-Benzobicyclo[ 2.2.2]octa-2,5,7-triene-2,3-dicarboxylate. *Acta Crystallogr., Sect. C: Struct. Chem.* **1989,** *C45*, 1250-1251.
85. Pokkuluri, P. R.; Scheffer, J. R.; Trotter, J., Dimethyl 9-Phenyl-1,4-dihydro-1,4-ethenoanthracene-11,12-dicarboxylate. *Acta Crystallogr., Sect. C: Struct. Chem.* **1994,** *C50*, 415-417.
86. Banwell, M.; Dupuche, J.; Gable, R., A Caveat Concerning Anionic Oxy-cope Rearrangements Within Bicyclo[2.2.2]octenyl Frameworks. *Aust. J. Chem.* **1996,** *49* (5), 639-645.
87. Dopp, D.; Memarian, H. R.; Kruger, C.; Raabe, E., 1,4-Photoaddition of (alpha)-(tert-Butylthio)acrylonitrile to Acylnaphthalenes. *Chem. Ber.* **1989,** *122*, 585-588.
88. Bodrikov, I. V.; Shebelova, I. Y. U.; Gatilov, Y. V.; Rybalova, T.; Tatarova, L.; Barkhash, V., New Reaction of SCl2 with Tetrafluorobenzobarrelene. *ChemInform* **1996,** *27* (2).
89. Lee, G.-A.; Cherng, C.-H.; Huang, A. N.; Lin, Y.-H., Synthesis and chemistry of tricyclic cyclopropene-tricyclo[3.2.2.02,4]nona-2(4),6-diene. *Tetrahedron* **2003,** *59* (9), 1539-1545.
90. Trindle, C.; Wolfskill, T., Substituent effects on the geometry of the cyclooctatetraene ring. *J. Org. Chem.* **2002,** *56* (18), 5426-5436.
91. Cremer, D., A General Definition of Ring Substituent Positions. *Isr. J. Chem.* **1980,** *20*, 12-19.
92. Cremer, D.; Pople, J. A., A General Definition of Ring Puckering Coordinates. *J. Am. Chem. Soc.* **1975**, 1354-1358.

93. Li, W.-K.; Chiu, S.-W.; Mak, T. C. W., Semi-empirical molecular orbital conformational study of benzannelated cyclooctatetraenes and related compounds, and X-ray crystal structure of benzocyclooctatetraene. *J. Mol. Struct.* **1983,** *94*, 285-291.
94. Bohshar, M.; Maas, G.; Heydt, H.; Regitz, M., Untersuchungen an Diazoverbindungen und Aziden-Li. *Tetrahedron* **1984,** *40* (24), 5171-5176.
95. Berno, P.; Ceccon, A.; Gambaro, A.; Venzo, A.; Ganis, P.; Valle, G., Synthesis, Structure, and Haptotropic Rearrangement of Benzocyclooctatetraenetricarbonylchromium(0) Complexes. *J. Chem. Soc. Perkin Trans. II* **1987**, 935-941.
96. Bender, C. O.; Boeré, R. T., (5Z,7Z,9Z)-5,10-Di-bromo-benzo[8]annulene. *Acta Crystallogr., Sect. E: Crystallogr. Commun.* **2013,** *69* (11), o1641.
97. Uoyama, H.; Ono, N.; Uno, H., Preparation of Biphenylene- and Benzocyclooctene-Fused Heterocycles. *Heterocycles* **2007,** *72* (1), 363-372.
98. Clar, E.; Schoental, R., *Polycyclic Hydrocarbons*. Springer-Verlag, Berlin, Heidelberg: 1964; Vol. 2.
99. Linden, A.; Chen, Y.; Hansen, H. J., Experimental Crystal Structure Determination. *CSD Communication (Private Communication)* **2018**.
100. Poppleton, B. J., Photochemical reaction products. CI: 8b-methoxy-l,3-diphenyl-2a,8bdihydrocyclobuta[a]naphthalene. CII: 8b-methoxy-2,3-diphenyl-2a,8bdihydrocyclobuta[a]naphthalene. *J. Cryst. Mol. Struct.* **1980,** *10* (5/6), 103-113.
101. Jones, P. G.; Kennard, O.; Sheldrick, G. M., Crystal and Molecular Structure of 2a,3,4,5,6,7,8,8b-Octafluoro-2-methyl-2-( 2-methylprop-1-enyl)-1,2,2a,8b-tetrahydrocyclobuta[a]napthalene. *J. Chem. Soc. Perkin Trans. II* **1977**, 1985-1989.
102. Bowman, R. M.; Calvo, C.; McCullough, J. J.; Miller, R. C.; Singh, I., The Photo-addition of Naphthalene and Acrylonitrile. An X-ray and Nuclear Magnetic Resonance Study of the Cycloadducts. *Can. J. Chem.* **1973,** *51*, 1060-1067.
103. Memarian, H. R.; Nasr-Esfahani, M.; Boese, R.; Dopp, D., Photoaddition of 2-Morpholinoacrylonitrile to Substituted 1-Acetonaphthones. *Liebigs Ann./Recl.* **1997**, 1023-1027.
104. Al-Jalal, N. A.; Pritchard, R. G.; McAuliffe, C. A., Light-induced [2 + 2] Cycloaddition of 6-Methoxy-2-naphthonitrile to 2-Chloroacrylonitrile. *J. Chem. Res.* **1999,** *23* (1), xiv.
105. Dolomanov, O. V.; Bourhis, L. J.; Gildea, R. J.; Howard, J. A. K.; Puschmann, H., OLEX2: a complete structure solution, refinement and analysis program. *J. Appl. Crystallogr.* **2009,** *42* (2), 339-341.
106. Neese, F., Software update: the ORCA program system, version 4.0. *Wiley Interdiscip. Rev.: Comput. Mol. Sci.* **2017,** *8*, e1327.
107. Neese, F., The ORCA program system. *Wiley Interdiscip. Rev.: Comput. Mol. Sci.* **2012,** *2*, 73-78.
108. Cromer, D. T.; Waber, J. T., *International Tables for X-Ray Crystallography* **1974,** *IV*, 71.
109. Spek, A. L., Structure validation in chemical crystallography. *Acta Crystallogr., Sect. D: Biol. Crystallogr.* **2009,** *65* (2), 148-55.
110. Spek, A. L., Single-crystal structure validation with the program PLATON. *J. Appl. Cryst.* **2002,** *36*, 7-13.
111. Thompson, A. L., Chemical Crystallography: when are ‘ bad data’ ‘good data’? *Crystallography Reviews* **2019,** *25* (1), 3-53.
112. Allen, F. H.; Bruno, I. J., Bond lengths in organic and metal-organic compounds revisited: X-H bond lengths from neutron diffraction data. *Acta Crystallogr., Sect. B: Struct. Sci., Cryst. Eng. Mater.* **2010,** *66* (3), 380-6.
113. Dunitz, J. D., Intermolecular atom-atom bonds in crystals? *IUCrJ* **2015,** *2* (2), 157-8.
114. Lecomte, C.; Espinosa, E.; Matta, C. F., On atom-atom 'short contact' bonding interactions in crystals. *IUCrJ* **2015,** *2* (2), 161-3.
115. First, J. T.; Slocum, J. D.; Webb, L. J., Quantifying the Effects of Hydrogen Bonding on Nitrile Frequencies in GFP: Beyond Solvent Exposure. *J. Phys. Chem. B* **2018,** *122* (26), 6733-6743.

116. Luschtinetz, R.; Gemming, S.; Seifert, G., Theoretical study on the CH···NC hydrogen bond interaction in thiophene-based molecules. *Comput. Theor. Chem.* **2013,** *1005*, 45-52.
117. Thakur, T. S.; Dubey, R.; Desiraju, G. R., Intermolecular atom-atom bonds in crystals - a chemical perspective. *IUCrJ* **2015,** *2* (2), 159-60.
118. Sheldrick, G. M., A short history of SHELX. *Acta Crystallogr A* **2008,** *64* (Pt 1), 112-122.
119. Sheldrick, G., SHELXT - Integrated space-group and crystal-structure determination. *Acta Crystallogr., Sect. A: Found. Adv.* **2015,** *71* (1), 3-8.
120. Neese, F., Software update: The ORCA program system—Version 5.0. *WIREs Computational Molecular Science* **2022,** *12* (5), e1606.
121. Novelli, G.; McMonagle, C. J.; Kleemiss, F.; Probert, M.; Puschmann, H.; Grabowsky, S.; Maynard-Casely, H. E.; McIntyre, G. J.; Parsons, S., Accurate H-atom parameters for the two polymorphs of L-histidine at 5, 105 and 295 K. *Acta Crystallographica Section B Structural Science, Crystal Engineering and Materials* **2021,** *77* (5), 785-800.

## *For Table of Contents Use Only*

TOC Graphic and Text – this is prepared to the 'actual size' for printing, 6 x 3.5 cm at 600 d.p.i.